**SUPPLEMENTAL INFORMATION**

# CARM1 Inhibition Enables Immunotherapy of Resistant Tumors by Dual Action on Tumor and T-cells

Sushil Kumar[1,2*], Zexian Zeng[3*], Archis Bagati[1,2*], Rong En Tay[1,2*], Lionel A. Sanz[4], Stella R. Hartono[4], Yoshinaga Ito[1,2], Fieda Abderazzaq[5,6], Elodie Hatchi[5,6], Peng Jiang[3,7], Adam N. R. Cartwright[1,2], Olamide Olawoyin[1,8], Nathan D. Mathewson[1,2], Jason W. Pyrdol[1,2], Mamie Z. Li[9], John G. Doench[10], Matthew A. Booker[11], Michael Y. Tolstorukov[11], Stephen J. Elledge[9], Frédéric Chédin[4], X. Shirley Liu[3#], Kai W. Wucherpfennig[1,2,12#]

Figure S1

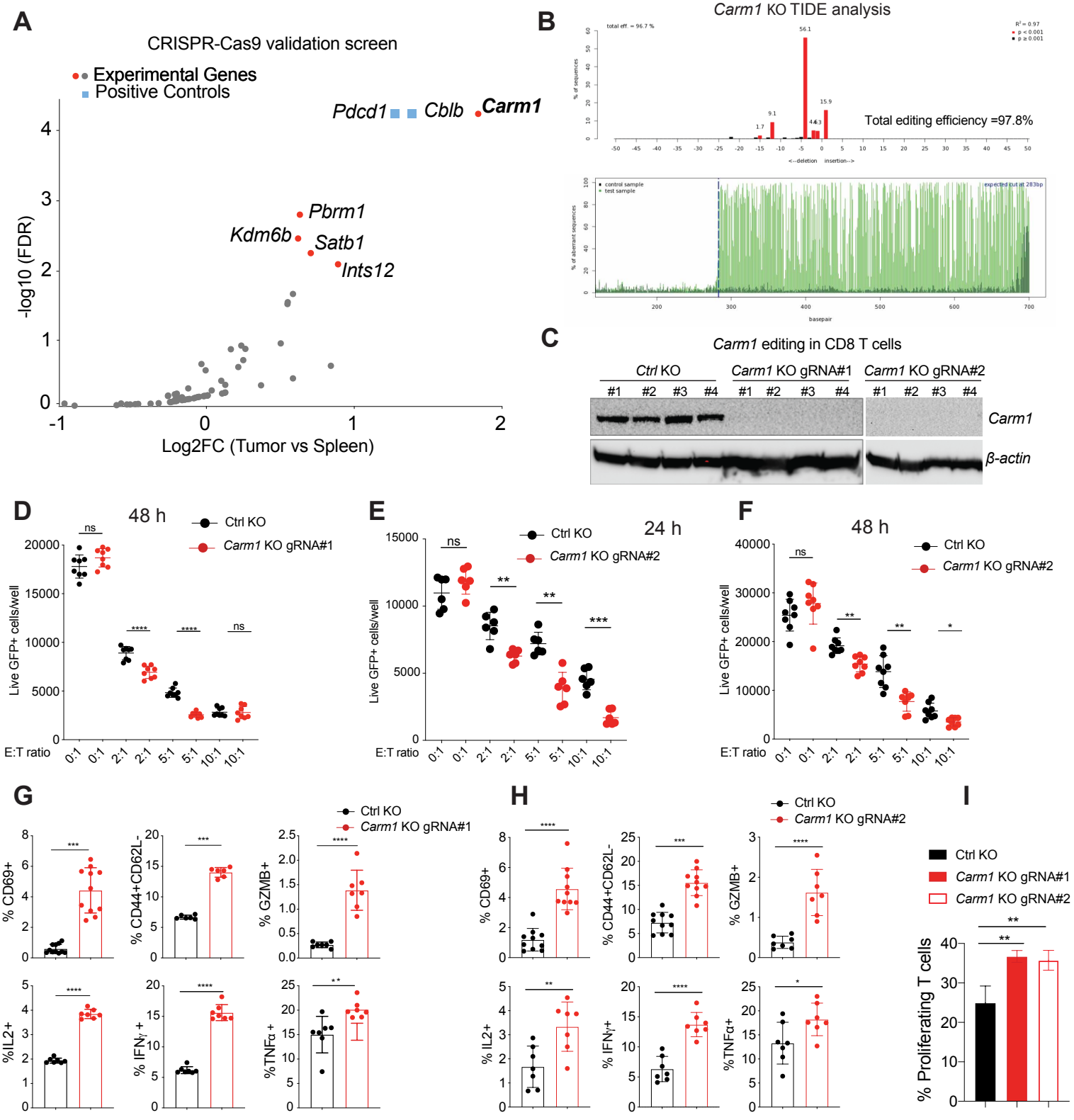
A
CRISPR-Cas9 validation screen
Experimental Genes
Positive Controls
Pdcd1
Cblb
Carm1
Pbrm1
Kdm6b
Satb1
Ints12
-log10 (FDR)
Log2FC (Tumor vs Spleen)
B
Carm1 KO TIDE analysis
Total editing efficiency =97.8%
C
Carm1 editing in CD8 T cells
Ctrl KO
Carm1 KO gRNA#1
Carm1 KO gRNA#2
Carm1
β-actin
D
48 h
Ctrl KO
Carm1 KO gRNA#1
Live GFP+ cells/well
E:T ratio
E
24 h
Carm1 KO gRNA#2
F
48 h
G
H
I
% CD69+
% CD44+CD62L-
% GZMB+
%IL2+
% IFNγ +
%TNFα +
% IL2+
% IFNγ+
%TNFα+
% Proliferating T cells

**Figure S1. Identification of CARM1 as a therapeutic target in tumor-infiltrating T cells and tumor cells. Related to Figure 1.**

**A.** Validation screen with focused epigenetic gRNA library. The library contained gRNAs for the top 31 genes from the primary screen and two positive control genes (*Pdcd1* and *Cblb*); 186 gRNAs were added as controls. OT-I T cells were transduced with the lentiviral gRNA library and injected into mice with subcutaneous B16F10-OVA tumors. On day 10 following T cell transfer, gRNA representation was quantified for T cells isolated from tumors (experimental organ) versus spleens (control organ). Graph shows log2 fold difference in gRNA representation in tumors versus spleens (X-axis) and statistical significance for indicated genes (Y-axis).

**B.** Validation of *Carm1* KO in CD8 T cells by CRISPR. TIDE analysis (Tracking of Indels by Decomposition) of genomic DNA sequenced from KO cells showing 97.8% editing efficiency.

**C.** Western blot analysis of Carm1 protein in OT-I CD8 T cells edited with control or *Carm1* gRNAs (2 different *Carm1* gRNAs, 4 technical replicates in each group). CD8 T cells were electroporated with RNPs composed of Cas9 protein with bound gRNAs; Carm1 protein levels were analyzed on day 7 following electroporation.

**D.** T cell cytotoxicity assay with *Carm1*-KO (*Carm1* gRNA#1) and control-KO OT-I CD8 T cells. T cells were co-cultured with B16F10-OVA-ZsGreen tumor cells at indicated effector to target (E: T) ratios (n=7-10/replicates per condition); 48 hours later live GFP-positive tumor cells were counted using a Celigo image cytometer. Data are representative of three experiments and shown as mean ± SEM. ****$p < 0.0001$, by unpaired two-sided Mann-Whitney test.

**E-F.** T cell cytotoxicity assay with *Carm1*-KO (*Carm1* gRNA#2) and control-KO OT-I CD8 T cells. 24 **(E)** and 48 **(F)** hours later live GFP-positive tumor cells were counted using a Celigo image cytometer.

**G-H.** Flow cytometry analysis of *Carm1*-KO CD8 T cells generated using gRNA#1 **(G)**, gRNA#2

**(H)** and control-KO OT-I CD8 T cells following co-culture with tumor cells. Edited T cells were co-cultured with B16-OVA-Zsgreen tumor cells at a 1:2 ratio for 24 hours followed by flow cytometric analysis of indicated markers. Data are representative of two experiments and shown as mean ± SEM, ** p< 0.01, ***p < 0.001, ****p < 0.0001 by unpaired two-sided Mann-Whitney test.

**I.** Assay to examine antigen-dependent proliferation of control-KO or *Carm1*-KO CD8 T cells. OT-I CD8 T cells were edited with control or *Carm1* gRNAs (gRNA#1 or #2) and cultured for 5 days in the presence of IL-15 and IL-7. T cells were then co-cultured for 4 days with B16-OVA-ZsGreen cells at a 5:1 (E:T) ratio, and CTV dilution was assessed by flow cytometry. Data were summarized as mean ± S.E.M. and analyzed by unpaired two-sided Mann-Whitney test. **p < 0.01, ****p < 0.0001.

Figure S2

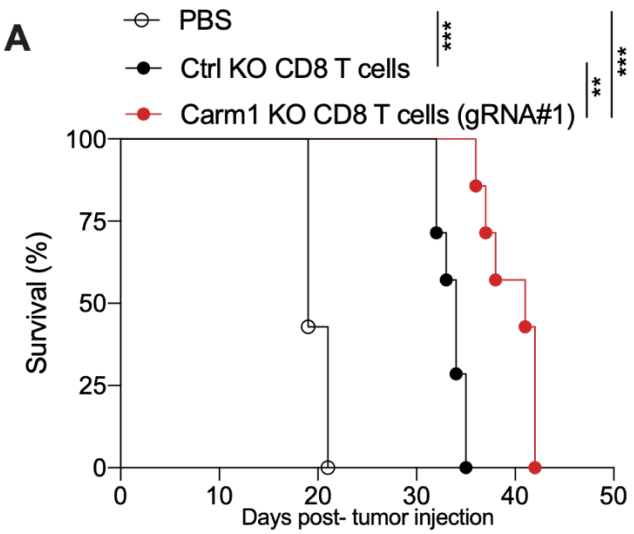
A
PBS
Ctrl KO CD8 T cells
Carm1 KO CD8 T cells (gRNA#1)
***
**
***
Survival (%)
100
75
50
25
0
0
10
20
30
40
50
Days post- tumor injection

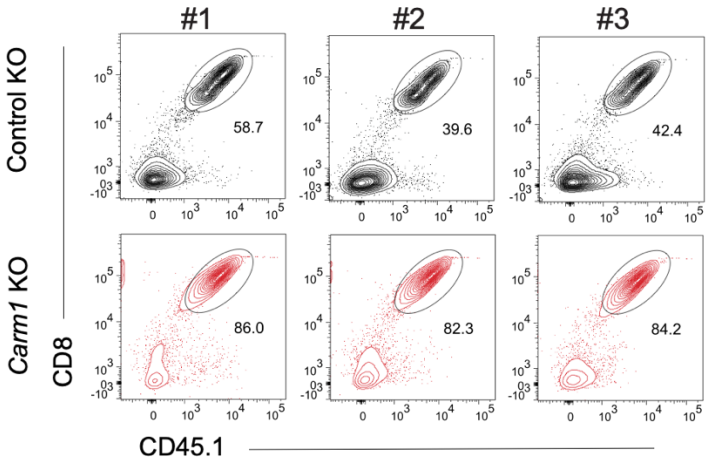
B
#1
#2
#3
Control KO
Carm1 KO
CD8
58.7
39.6
42.4
86.0
82.3
84.2
CD45.1

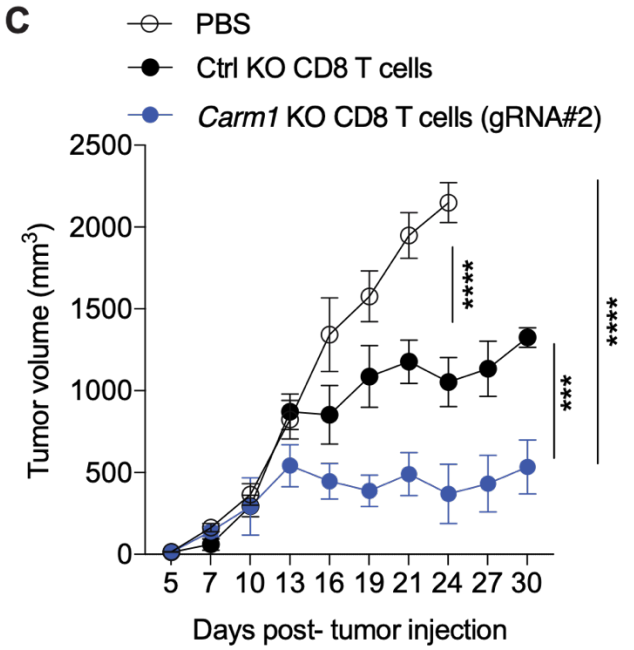
C
PBS
Ctrl KO CD8 T cells
Carm1 KO CD8 T cells (gRNA#2)
Tumor volume (mm3)
2500
2000
1500
1000
500
0
****
***
****
5 7 10 13 16 19 21 24 27 30
Days post- tumor injection

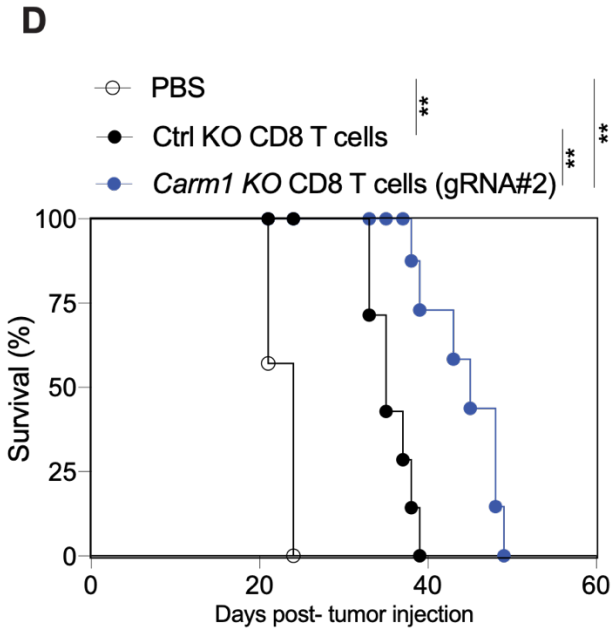
D
PBS
Ctrl KO CD8 T cells
Carm1 KO CD8 T cells (gRNA#2)
**
**
**
Survival (%)
100
75
50
25
0
0
20
40
60
Days post- tumor injection

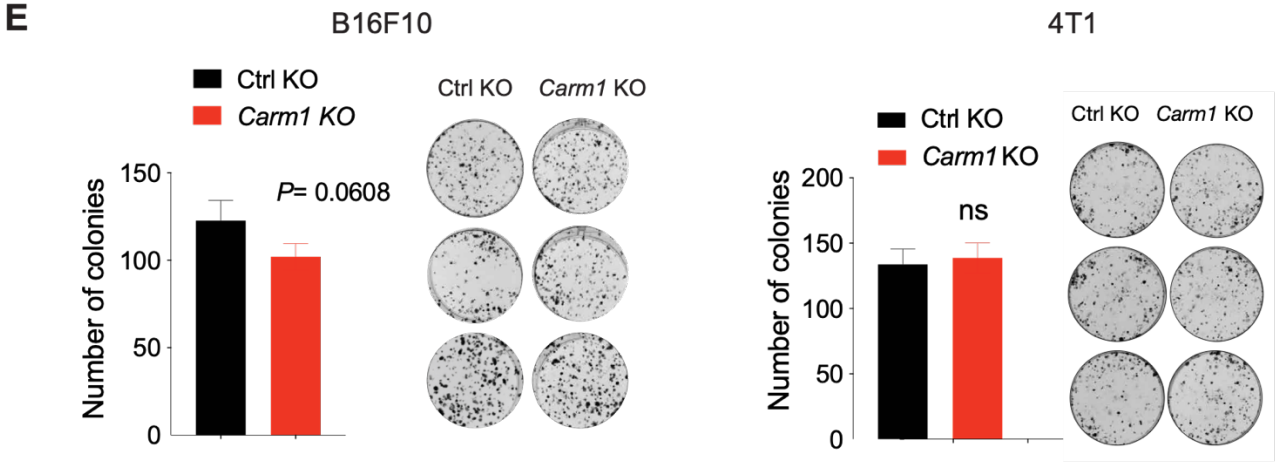
E
B16F10
Ctrl KO
Carm1 KO
P= 0.0608
Number of colonies
150
100
50
0
Ctrl KO
Carm1 KO
4T1
Ctrl KO
Carm1 KO
ns
Number of colonies
200
150
100
50
0
Ctrl KO
Carm1 KO

**Figure S2. Inactivation of *Carm1* in CD8 T cells enhances their anti-tumor function. Related to Figure 1.**

**A.** Survival of mice with B16F10-Ova melanomas following adoptive transfer of *Carm1*-KO (generated using gRNA#1) or control-KO OT-I CD45.1 CD8 T cells.

**B.** Representative flow plots of tumor infiltrating CD45.1 CD8 T cells following adoptive transfer of *Carm1*-KO or control-KO OT-I CD45.1 CD8 T cells. Gated on Live/singlets/CD45+ cells.

**C.** Anti-tumor activity of adoptively transferred *Carm1*-KO (generated using gRNA#2) or control-KO OT-I CD45.1 CD8 T cells. B16-OVA-ZsGreen tumor cells ($0.1x10^6$) were implanted subcutaneously. On day 7 following tumor cell inoculation, edited CD8 T cells ($1x10^6$) were transferred via tail vein injection. Tumor size was recorded; n=8-10 mice per group.

**D.** Survival of mice with B16F10-Ova melanomas following adoptive transfer of *Carm1*-KO (generated using gRNA#2) or control-KO OT-I CD45.1 CD8 T cells.

**E.** Growth of *Carm1*-KO and control-KO B16F10 melanoma cells (left) and 4T1 breast cancer cells (right) in a colony formation assay (500 input cells/well, 6-well plates for 5 days). Quantification of number of colonies in each group and representative images of plates of colonies are shown for each condition. Data are representative of two independent experiments.

Figure S3

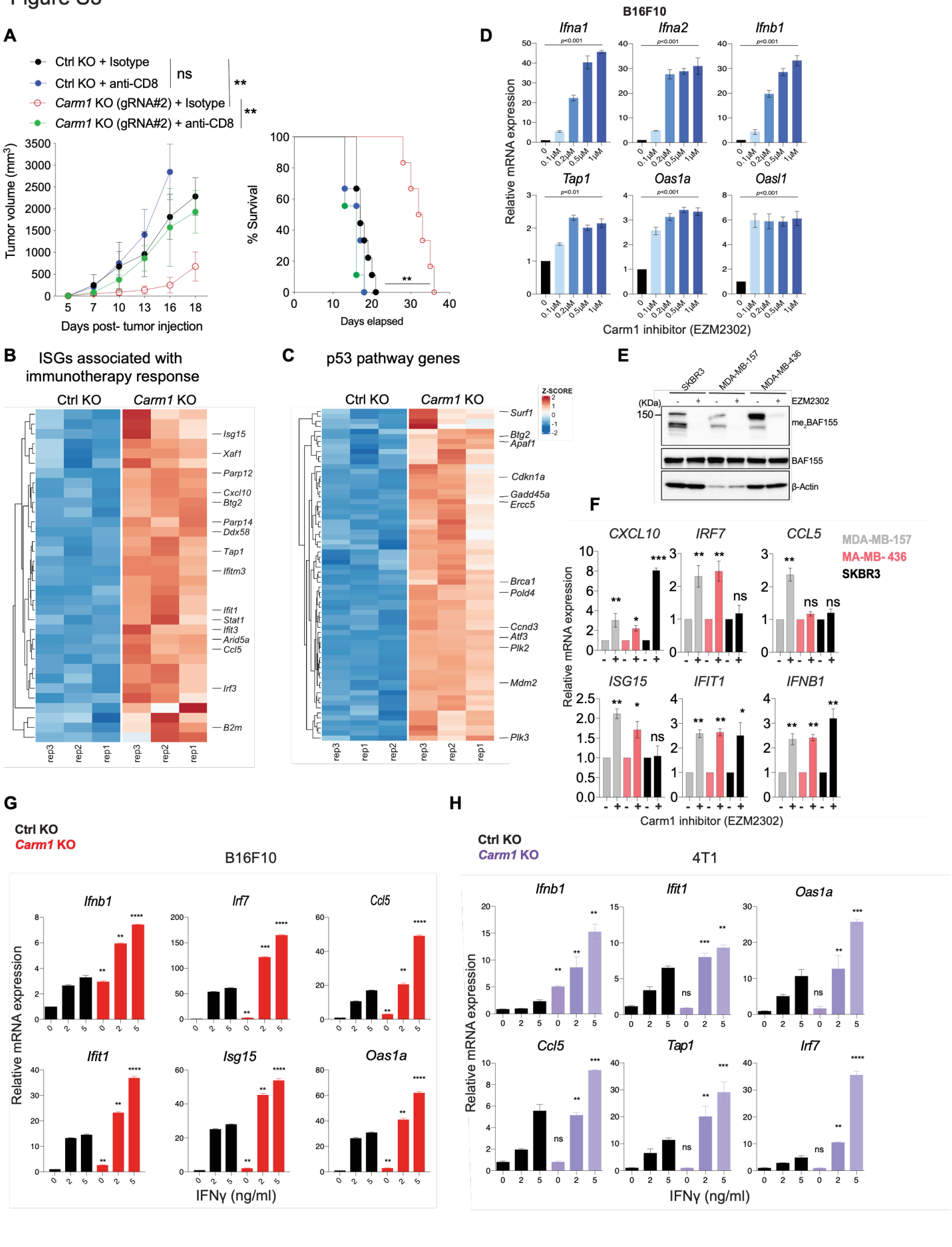
A
Ctrl KO + Isotype
Ctrl KO + anti-CD8
Carm1 KO (gRNA#2) + Isotype
Carm1 KO (gRNA#2) + anti-CD8
ns
**
**
Tumor volume (mm3)
Days post- tumor injection
% Survival
Days elapsed
B16F10
D
Ifna1
Ifna2
Ifnb1
Tap1
Oas1a
Oasl1
Relative mRNA expression
Carm1 inhibitor (EZM2302)
B
ISGs associated with immunotherapy response
Ctrl KO
Carm1 KO
Isg15
Xaf1
Parp12
Cxcl10
Btg2
Parp14
Ddx58
Tap1
Ifitm3
Ifit1
Stat1
Ifit3
Arid5a
Ccl5
Irf3
B2m
rep3
rep2
rep1
C
p53 pathway genes
Z-SCORE
Surf1
Btg2
Apaf1
Cdkn1a
Gadd45a
Ercc5
Brca1
Pold4
Ccnd3
Atf3
Plk2
Mdm2
Plk3
E
SKBR3
MDA-MB-157
MDA-MB-436
(KDa)
150
EZM2302
me2BAF155
BAF155
β-Actin
F
CXCL10
IRF7
CCL5
ISG15
IFIT1
IFNB1
MDA-MB-157
MA-MB- 436
SKBR3
Relative mRNA expression
Carm1 inhibitor (EZM2302)
G
Ctrl KO
Carm1 KO
B16F10
Ifnb1
Irf7
Ccl5
Ifit1
Isg15
Oas1a
Relative mRNA expression
IFNγ (ng/ml)
H
Ctrl KO
Carm1 KO
4T1
Ifnb1
Ifit1
Oas1a
Ccl5
Tap1
Irf7
Relative mRNA expression
IFNγ (ng/ml)

**Figure S3. Targeting of *Carm1* induces a type I interferon response in human and murine tumor cells. Related to Figures 3 and 4.**

**A.** Growth of *Carm1*-KO (*Carm1* gRNA#2) and control-KO B16F10 tumors (left) and survival of tumor bearing mice (right). Mice (n=8-10/group) were treated with CD8 depleting or isotype control antibodies.

**B.** Heatmap of differentially expressed ISGs in *Carm1*-KO and control-KO B16F10 tumor cells (n=3/group) that were previously found to be associated with immunotherapy response in human melanoma (Benci et al., 2019). Data are representative of two independent experiments.

**C.** Heatmap of differentially expressed p53 pathway genes in *Carm1*-KO versus control-KO B16F10 tumor cells (n=3/group). Data are representative of two independent experiments.

**D.** RT-qPCR analysis of indicated ISGs in B16F10 cells treated with CARM1 inhibitor EZM2302 (0 – 1 μM) for 7 days (n=3/group).

**E.** Western blot analysis to validate activity of CARM1 inhibitor (EZM2302) in human tumor cells. BAF155 is a well-validated target of CARM1. SKBR3, MDA-MB-157 and MDA-MB-436 cells were treated with EZM2302 (0.1 μM) or solvent control for 24 hours. Western blots were probed with Abs specific for di-methylated BAF155 protein (me2BAF155), total BAF155 protein and β-actin (loading control).

**F.** Analysis of ISGs in human tumor cells treated with CARM1 inhibitor (EZM2302). RT-qPCR analysis of selected ISGs and IFNs in human SKBR3, MDA-MB-157 and MDA-MB-436 cells treated with vehicle or CARM1 inhibitor (2 μM) for 7 days (n=3/group).

**G.** Responsiveness of *Carm1*-KO compared to control-KO B16F10 cells to IFNγ treatment. Cells were treated overnight with IFNγ (0, 2 or 5 ng/ml), and mRNA levels of ISGs were analyzed by RT-qPCR (n=3/group).

**H.** Responsiveness of *Carm1*-KO compared to control-KO 4T1 cells to IFNγ treatment. Cells were treated overnight with IFNγ (0, 2 or 5 ng/ml), and mRNA levels of ISGs were analyzed by RT-qPCR (n=3/group).

Figure S4

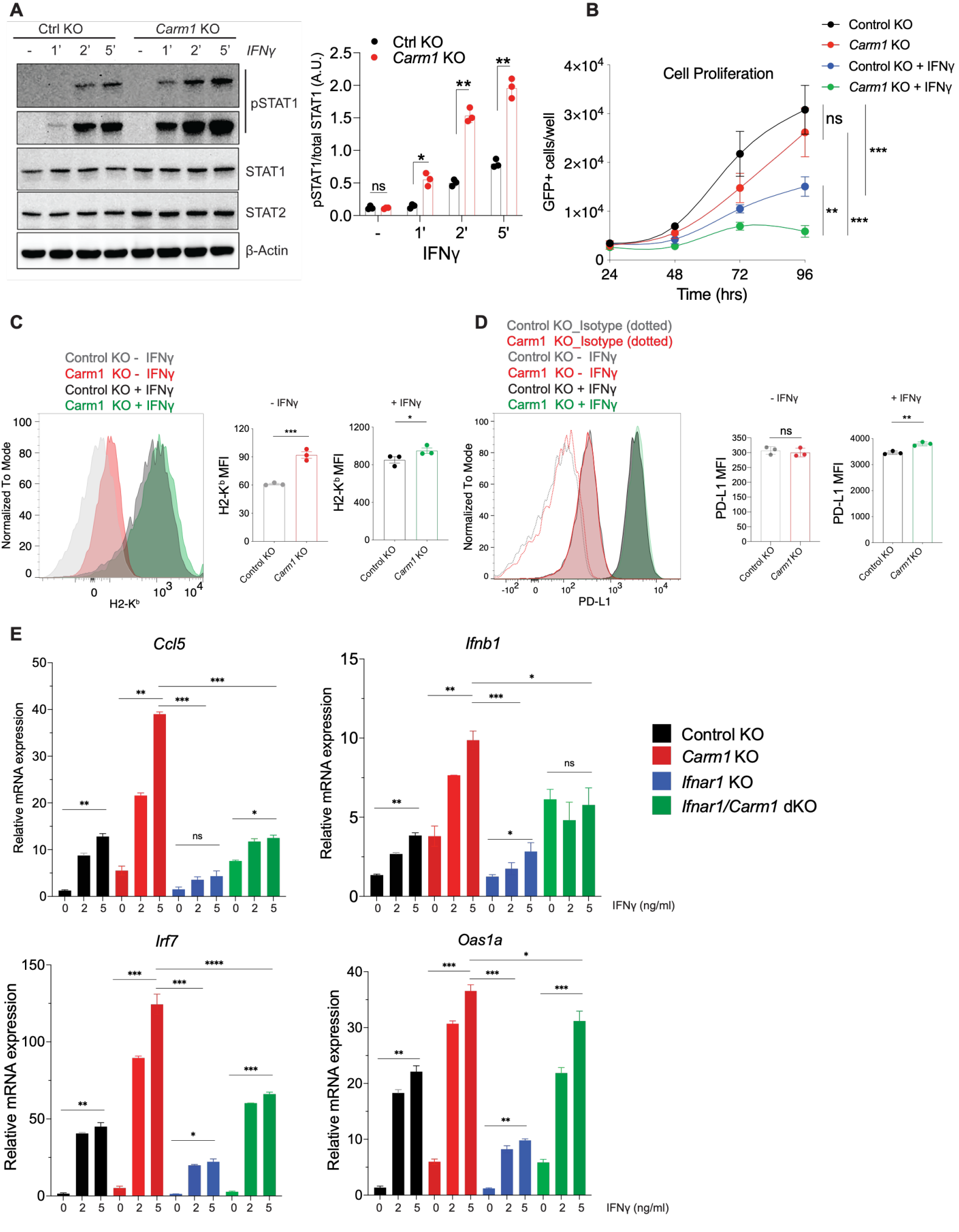
A
Ctrl KO
Carm1 KO
- 1' 2' 5' - 1' 2' 5'
IFNγ
pSTAT1
STAT1
STAT2
β-Actin
Ctrl KO
Carm1 KO
pSTAT1/total STAT1 (A.U.)
IFNγ
B
Control KO
Carm1 KO
Control KO + IFNγ
Carm1 KO + IFNγ
Cell Proliferation
GFP+ cells/well
Time (hrs)
ns
C
Control KO - IFNγ
Carm1 KO - IFNγ
Control KO + IFNγ
Carm1 KO + IFNγ
Normalized To Mode
H2-Kb
- IFNγ
+ IFNγ
H2-Kb MFI
Control KO
Carm1 KO
D
Control KO_Isotype (dotted)
Carm1 KO_Isotype (dotted)
PD-L1
PD-L1 MFI
E
Ccl5
Ifnb1
Irf7
Oas1a
Relative mRNA expression
Control KO
Carm1 KO
Ifnar1 KO
Ifnar1/Carm1 dKO
IFNγ (ng/ml)

**Figure S4. Targeting of *Carm1* enhances sensitivity of tumor cells to IFNγ. Related to Figure 4.**

**A.** Analysis of IFNγ signaling in *Carm1*-KO and control-KO B16F10 cells. B16F10 cells were stimulated with IFNγ for 0-5 minutes, and levels of phosphorylated STAT1 (pSTAT1) as well as total STAT1, STAT2 and β-actin were analyzed by Western blotting. Long (5min) and short (1min) exposures of same blot are shown for pSTAT1 (left). Quantification of pSTAT1 blots using ImageJ from three separate experiments shown on right.

**B.** Analysis of cell proliferation of *Carm1*-KO and control-KO B16F10 cells in the presence of IFNγ. Equal numbers of GFP+ B16F10 cells were cultured in complete media supplemented with IFNγ for 4 days, and GFP+ live cells were counted each day using a Celigo image cytometer (n=4/group).

**C.** Analysis of H2-$K^b$ expression +/- IFNγ treatment of *Carm1*-KO and control-KO B16F10 cells.

**D.** Analysis of PD-L1 expression +/- IFNγ treatment of *Carm1*-KO and control-KO B16F10 cells.

**E.** RT-qPCR analysis of indicated ISGs following stimulation with the indicated concentrations of IFNγ in control-KO, *Carm1*-KO, *Ifnar1*-KO and *Ifnar1/Carm1* dKO B16F10 cells (n=3/group).

# Figure S5

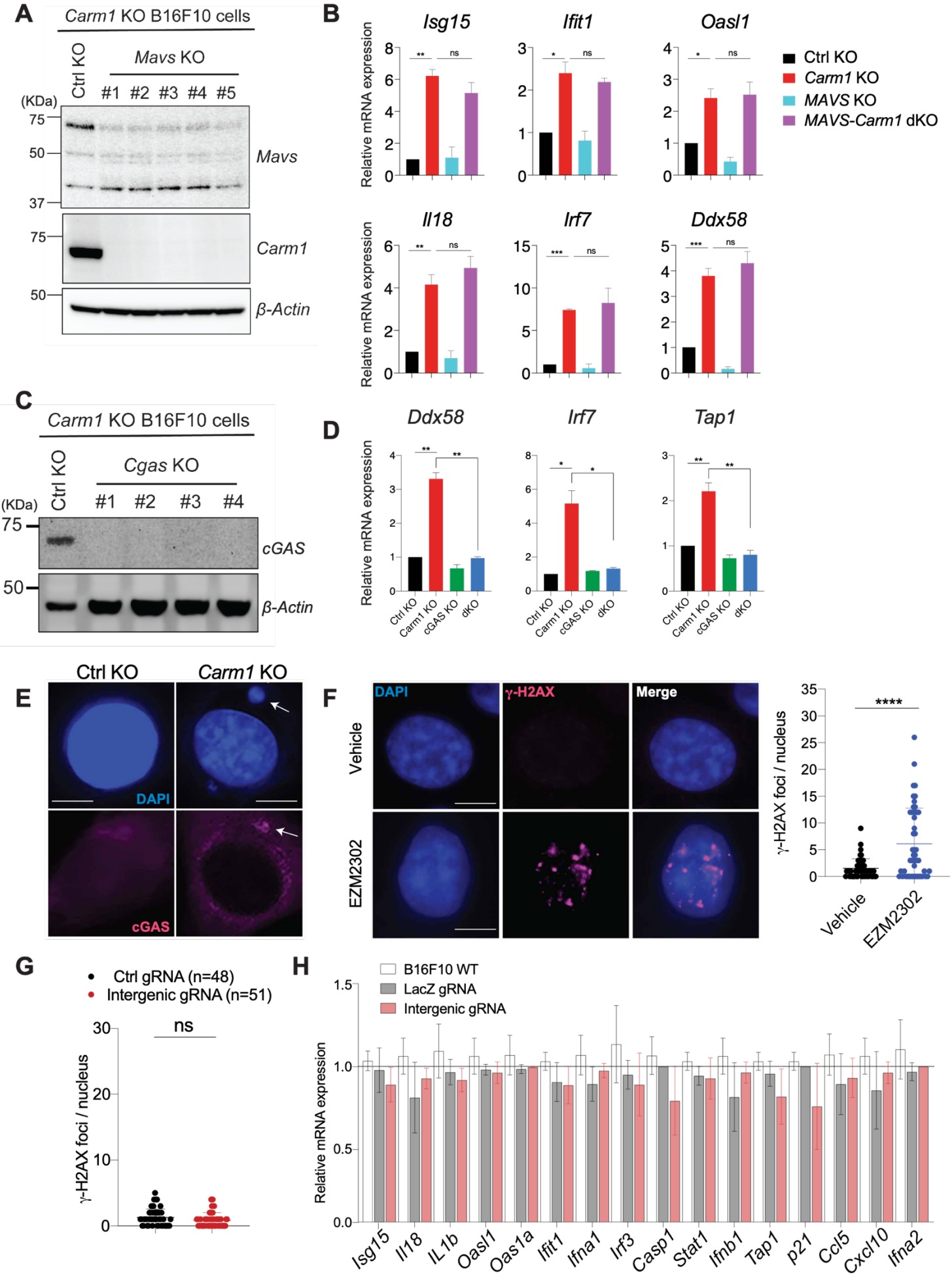
A
Carm1 KO B16F10 cells
Ctrl KO
Mavs KO
#1 #2 #3 #4 #5
(KDa)
75
50
37
75
50
Mavs
Carm1
β-Actin
B
Isg15
Ifit1
Oasl1
Il18
Irf7
Ddx58
Relative mRNA expression
Ctrl KO
Carm1 KO
MAVS KO
MAVS-Carm1 dKO
C
Carm1 KO B16F10 cells
Ctrl KO
Cgas KO
#1 #2 #3 #4
(KDa)
75
50
cGAS
β-Actin
D
Ddx58
Irf7
Tap1
Relative mRNA expression
Ctrl KO
Carm1 KO
cGAS KO
dKO
E
Ctrl KO
Carm1 KO
DAPI
cGAS
F
DAPI
γ-H2AX
Merge
Vehicle
EZM2302
γ-H2AX foci / nucleus
****
Vehicle
EZM2302
G
Ctrl gRNA (n=48)
Intergenic gRNA (n=51)
ns
γ-H2AX foci / nucleus
H
B16F10 WT
LacZ gRNA
Intergenic gRNA
Relative mRNA expression
Isg15
Il18
IL1b
Oasl1
Oas1a
Ifit1
Ifna1
Irf3
Casp1
Stat1
Ifnb1
Tap1
p21
Ccl5
Cxcl10
Ifna2

**Figure S5. Inactivation of *Carm1* induces a cGAS-mediated type I interferon response in human and murine tumor cells. Related to Figure 4.**

**A.** Mavs protein levels in *Carm1-KO* B16F10 cells edited with *Mavs or* control gRNAs. Replicates of different lines edited with the same gRNA are shown. β-actin is shown as a loading control.

**B.** RT-qPCR analysis of selected ISGs and IFNs in control, *Carm1*-KO, *Mavs*-KO and *Carm1/Mavs* dKO B16F10 cells (n=3/group).

**C.** cGas protein levels in *Carm1*-KO B16F10 cells edited with *Cgas* or control gRNAs. Replicates of different lines edited with the same *Cgas* gRNA or a control gRNA are shown. β-actin is shown as a loading control.

**D.** RT-qPCR analysis of selected ISGs in control, *Carm1*-KO, *Cgas*-KO and *Carm1/Cgas* dKO B16F10 cells (n=3/group).

**E.** Analysis of micronuclei in *Carm1*-KO and control-KO B16F10 cells. Tumor cells were transduced with a HA epitope tagged *Cgas* cDNA; ZsGreen was expressed downstream of an IRES by the same lentiviral vector. Representative immunofluorescence for HA epitope tagged cGAS (purple) and DAPI (blue); DAPI labeling was used to identify nuclei and micronuclei. Scale bar – 10μM.

**F.** dsDNA damage in CARM1 inhibitor (EZM2302) versus vehicle (5% Dextrose) treated B16F10 tumor cells based on labeling with γH2AX antibody. Representative immunofluorescence images (left) of γH2AX antibody labeling (purple); nuclei labeled with DAPI. Quantification of number of γH2AX foci/nucleus (right). Data are shown as mean ± SEM, ***$p < 0.001$, by unpaired two-sided Mann-Whitney test. Scale bar – 10μM.

**G.** Quantification of the percentage of B16F10 tumor cells with γH2AX foci following editing with two different control gRNAs (LacZ control gRNA, intergenic gRNA).

**H.** RT-qPCR analysis of ISGs in B16F10 cells without editing (WT) and following editing with two different control gRNAs (LacZ, intergenic). ISG levels were analyzed >7 days following editing.

Data shown in B, D, F and G are summarized as mean ± S.D. and were analyzed by unpaired two-sided Mann-Whitney test. Data are representative of three experiments, *$p < 0.05$, **$p < 0.01$, ***$p < 0.001$, ns (non-significant).

# Figure S6

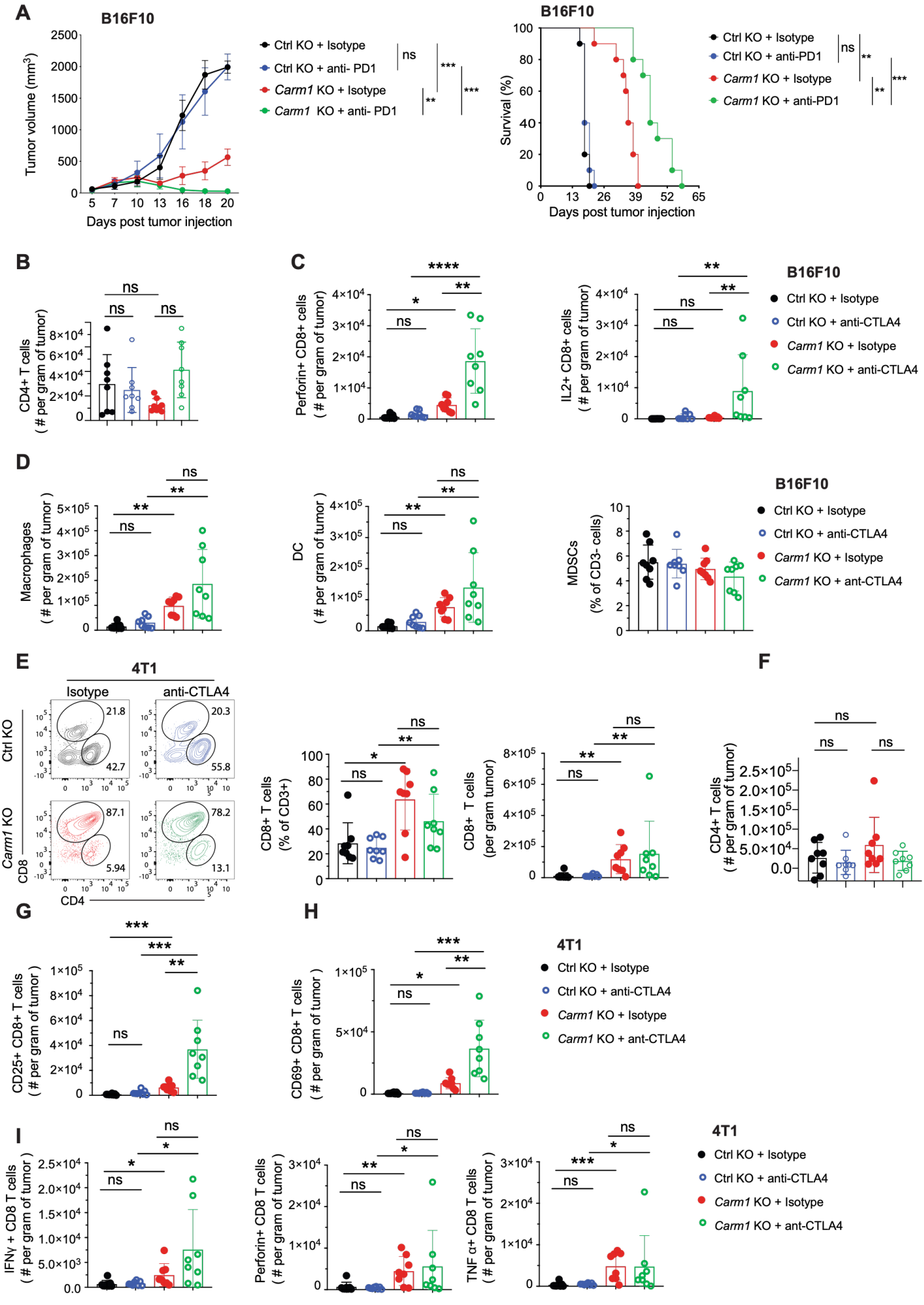
A
B16F10
Tumor volume (mm3)
Days post tumor injection
Ctrl KO + Isotype
Ctrl KO + anti- PD1
Carm1 KO + Isotype
Carm1 KO + anti- PD1
ns
**
***
***
B16F10
Survival (%)
Days post tumor injection
Ctrl KO + Isotype
Ctrl KO + anti-PD1
Carm1 KO + Isotype
Carm1 KO + anti-PD1
ns
**
**
***
B
CD4+ T cells ( # per gram of tumor)
C
Perforin+ CD8+ cells ( # per gram of tumor)
IL2+ CD8+ cells ( # per gram of tumor)
B16F10
Ctrl KO + Isotype
Ctrl KO + anti-CTLA4
Carm1 KO + Isotype
Carm1 KO + anti-CTLA4
D
Macrophages ( # per gram of tumor)
DC ( # per gram of tumor)
MDSCs (% of CD3- cells)
B16F10
Ctrl KO + Isotype
Ctrl KO + anti-CTLA4
Carm1 KO + Isotype
Carm1 KO + ant-CTLA4
E
4T1
Isotype
anti-CTLA4
Ctrl KO
Carm1 KO
CD8
CD4
21.8
42.7
20.3
55.8
87.1
5.94
78.2
13.1
CD8+ T cells (% of CD3+)
CD8+ T cells (per gram tumor)
F
CD4+ T cells ( # per gram of tumor)
G
CD25+ CD8+ T cells ( # per gram of tumor)
H
CD69+ CD8+ T cells ( # per gram of tumor)
4T1
Ctrl KO + Isotype
Ctrl KO + anti-CTLA4
Carm1 KO + Isotype
Carm1 KO + ant-CTLA4
I
IFNγ + CD8 T cells ( # per gram of tumor)
Perforin+ CD8 T cells ( # per gram of tumor)
TNF α+ CD8 T cells ( # per gram of tumor)
4T1
Ctrl KO + Isotype
Ctrl KO + anti-CTLA4
Carm1 KO + Isotype
Carm1 KO + ant-CTLA4

**Figure S6. *Carm1* inactivation sensitizes resistant tumors to treatment with CTLA-4 or PD-1 mAbs. Related to Figure 5.**

**A.** Treatment of *Carm1*-KO or control-KO B16F10 tumors with PD-1 or isotype control antibodies (n=8 mice/group). Tumor growth (left) and survival of tumor bearing mice (right) are shown.

**B.** Quantification of CD4 T cells (number per gram of tumor) in *Carm1*-KO and control-KO B16F10 tumors following treatment with anti-CTLA4 or control mAbs, n=8/group.

**C.** Number of intra-tumoral perforin+ CD8+ (left) and IL2+ CD8+ (right) T cells (per gram of tumor) in *Carm1*-KO and control-KO B16F10 tumors following treatment with anti-CTLA4 or control mAbs, n=8/group.

**D.** Number of intra-tumoral macrophages (live, singlet, CD45+ CD3- F4/80+) (left) and dendritic cells (DCs) (live, singlet, CD45+ CD3- F4/80- CD11c+ $MHCII^{hi}$) (middle) calculated per gram of tumor. Quantification of myeloid derived suppressor (MDSCs) (CD45+/CD3-/F4/80-/Gr1+, as percentage of CD3- cells) (right). Myeloid cells were analyzed in *Carm1*-KO and control-KO B16 tumors following treatment with anti-CTLA4 or control mAbs, n=8/group.

**E.** Analysis of *Carm1*-KO and control-KO 4T1 tumors following treatment with anti-CTLA4 or control mAbs. Contour plot show percentage of CD4 and CD8 positive intra-tumoral T cells (left). Quantification of percentage (middle) and number (right) of CD8+ T cells for indicated treatment groups.

**F.** Quantification of CD4+ T cells (number per gram of tumor) for indicated treatment groups in 4T1 tumor model.

**G.** Quantification of CD25+ intra-tumoral CD8+ T cells for indicated treatment groups in the 4T1 tumor model.

**H.** Quantification of CD69+ intra-tumoral CD8+ T cells for indicated treatment groups in the 4T1 tumor model.

**I.** Quantification of IFNγ (left), perforin (middle) and TNFα (right) positive intra-tumoral CD8+ T cells for indicated treatment groups in the 4T1 tumor model.

Data shown are representative of two independent experiments with 8 mice per group. No outliers were removed. Bar graphs represent data summarized as mean ± S.E.M and were analyzed by unpaired two-sided Mann-Whitney test, ****P < 0.0001; ***P < 0.001; **P < 0.01; *P < 0.05; n.s., non-significant.

Figure S7

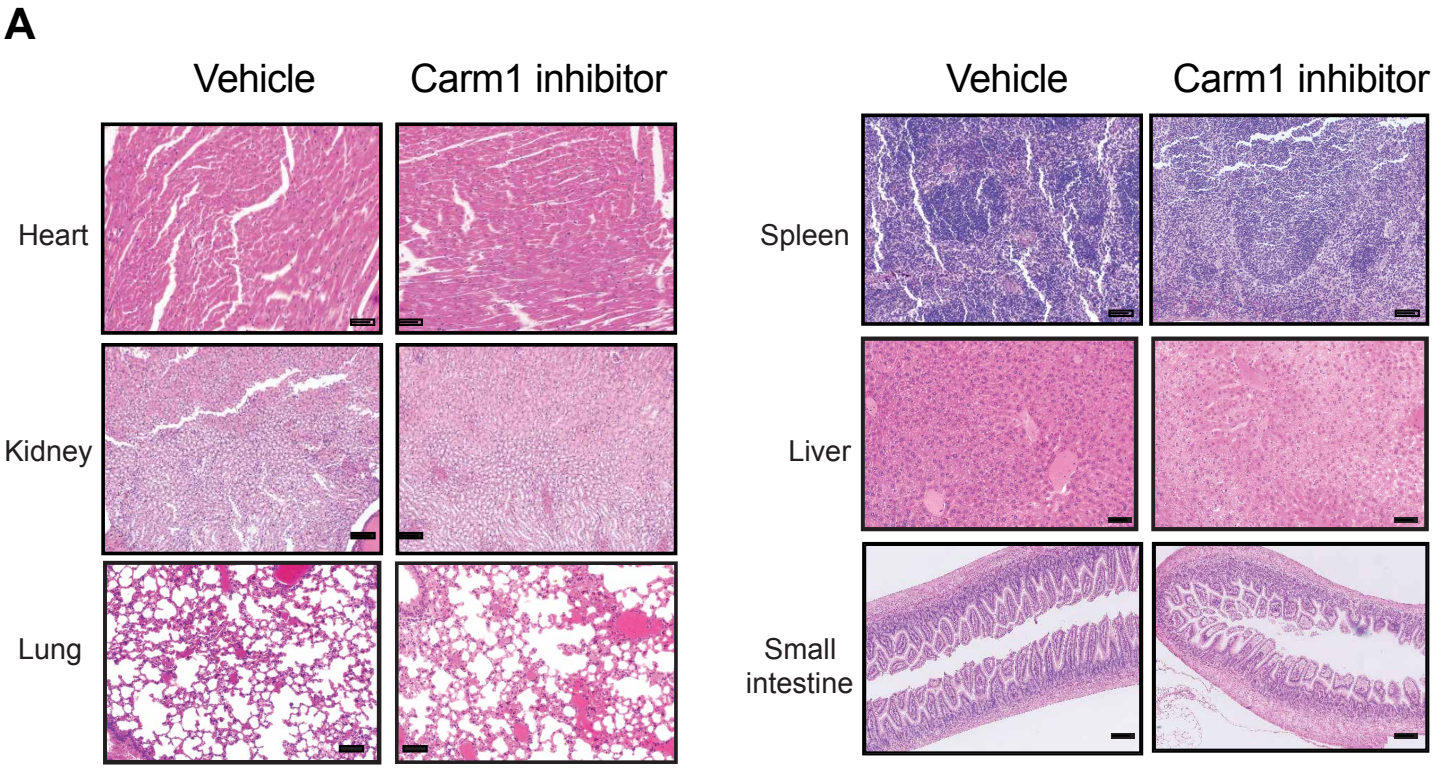
A
Vehicle
Carm1 inhibitor
Heart
Kidney
Lung
Vehicle
Carm1 inhibitor
Spleen
Liver
Small intestine

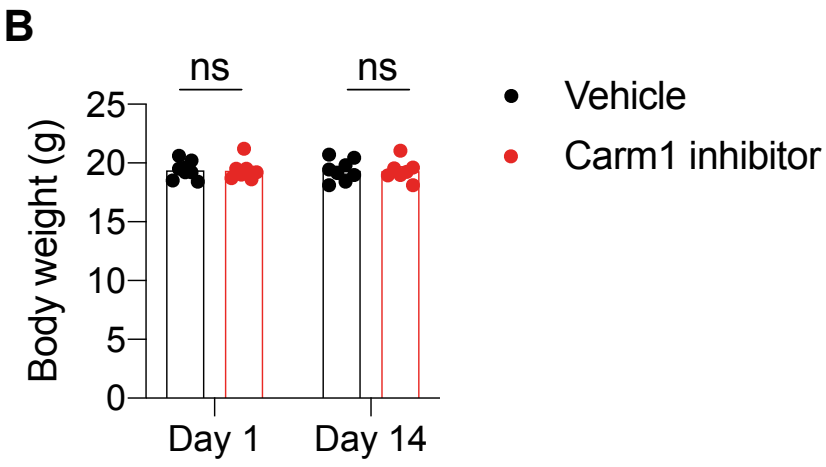
B
ns
ns
Body weight (g)
25
20
15
10
5
0
Day 1
Day 14
Vehicle
Carm1 inhibitor

**Figure S7. Evaluation of potential toxicity of Carm1 inhibitor (EZM2302) in C57Bl/6 mouse model. Related to Figure 5.**

**A.** Histopathological evaluation of major organs for assessment of potential toxicity of Carm1 inhibitor. Sex and age matched C57Bl/6 mice were randomized into two groups treated twice daily with either CARM1 inhibitor (150mg/kg) or vehicle via oral gavage for 14 days. Major organs including heart, spleen, kidney, liver, lung and small intestine were harvested for pathological assessment. Representative images of histopathological images (H&E stain) from vehicle or Carm1 inhibitor treated mice are shown (n=8/group). Scale bar = 50μM

**B.** Analysis of body weight of sex and age matched C57Bl/6 mice treated twice daily with CARM1 inhibitor (150mg/kg) or vehicle via oral gavage for 14 days (n=8/group).

Figure S8

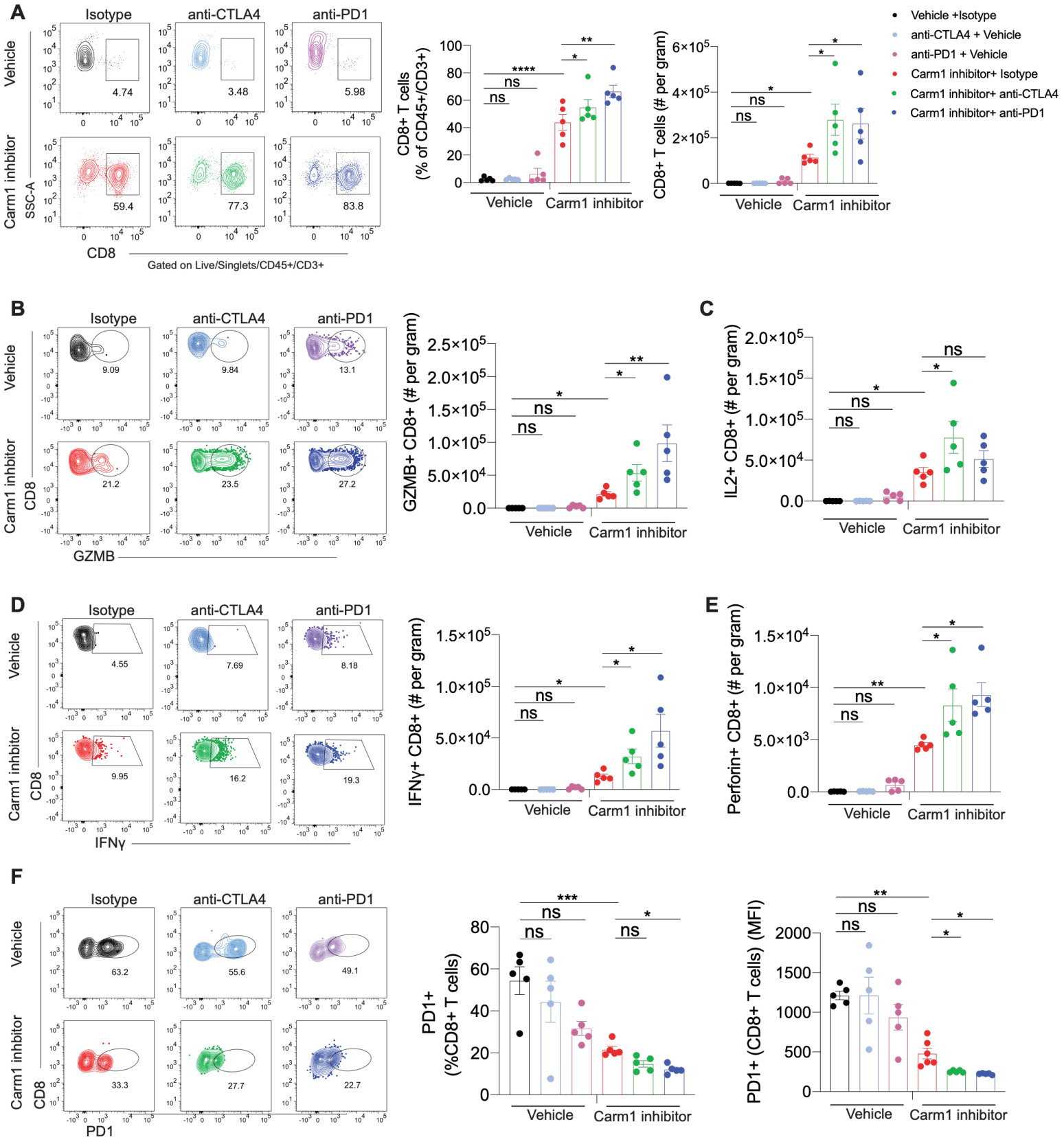
A
Isotype
anti-CTLA4
anti-PD1
Vehicle
Carm1 inhbitor
SSC-A
4.74
3.48
5.98
59.4
77.3
83.8
CD8
Gated on Live/Singlets/CD45+/CD3+
CD8+ T cells (% of CD45+/CD3+)
CD8+ T cells (# per gram)
Vehicle
Carm1 inhibitor
Vehicle +Isotype
anti-CTLA4 + Vehicle
anti-PD1 + Vehicle
Carm1 inhibitor+ Isotype
Carm1 inhibitor+ anti-CTLA4
Carm1 inhibitor+ anti-PD1
B
9.09
9.84
13.1
21.2
23.5
27.2
GZMB
GZMB+ CD8+ (# per gram)
C
IL2+ CD8+ (# per gram)
D
4.55
7.69
8.18
9.95
16.2
19.3
IFNγ
IFNγ+ CD8+ (# per gram)
E
Perforin+ CD8+ (# per gram)
F
63.2
55.6
49.1
33.3
27.7
22.7
PD1
PD1+ (%CD8+ T cells)
PD1+ (CD8+ T cells) (MFI)

**Figure S8. Changes in tumor microenvironment induced by monotherapy or combination therapy with CARM1 inhibitor. Related to Figure 5.**

**A.** Treatment of mice with B16F10 melanomas with CARM1 inhibitor or vehicle control. Mice also received isotype control, CTLA-4 or PD-1 mAbs, as indicated (n=5 mice/group). Representative flow plots of CD8 T cells gated on live/singlets/CD45+/CD3+ cells from indicated groups are shown on left. Quantification of CD8 T cells is shown as percentage of CD3+ T cells (middle) or number per gram of tumor (right) for the indicated treatment groups.

**B.** Number of intra-tumoral granzyme B+ CD8+ T cells per gram of tumor for the indicated treatment groups (n=5 mice/group). Representative flow plots are shown on left.

**C.** Number of intra-tumoral IL2+ CD8+ T cells per gram of tumor for the indicated treatment groups (n=5 mice/group).

**D.** Number of intra-tumoral IFNγ+ CD8+ T cells per gram of tumor for the indicated treatment groups (n=5 mice/group). Representative flow plots are shown on left.

**E.** Number of intra-tumoral perforin+ CD8+ T cells per gram of tumor for the indicated treatment groups (n=5 mice/group).

**F.** Analysis of intra-tumoral PD1+ CD8+ T cells (quantified as percentage of CD8+ T cells) for the indicated treatment groups (n=5 mice/group). Representative flow plots (left) and quantification of PD-1 expression as percentage of CD8 T cells (middle) or MFI (right) are shown.

Figure S9

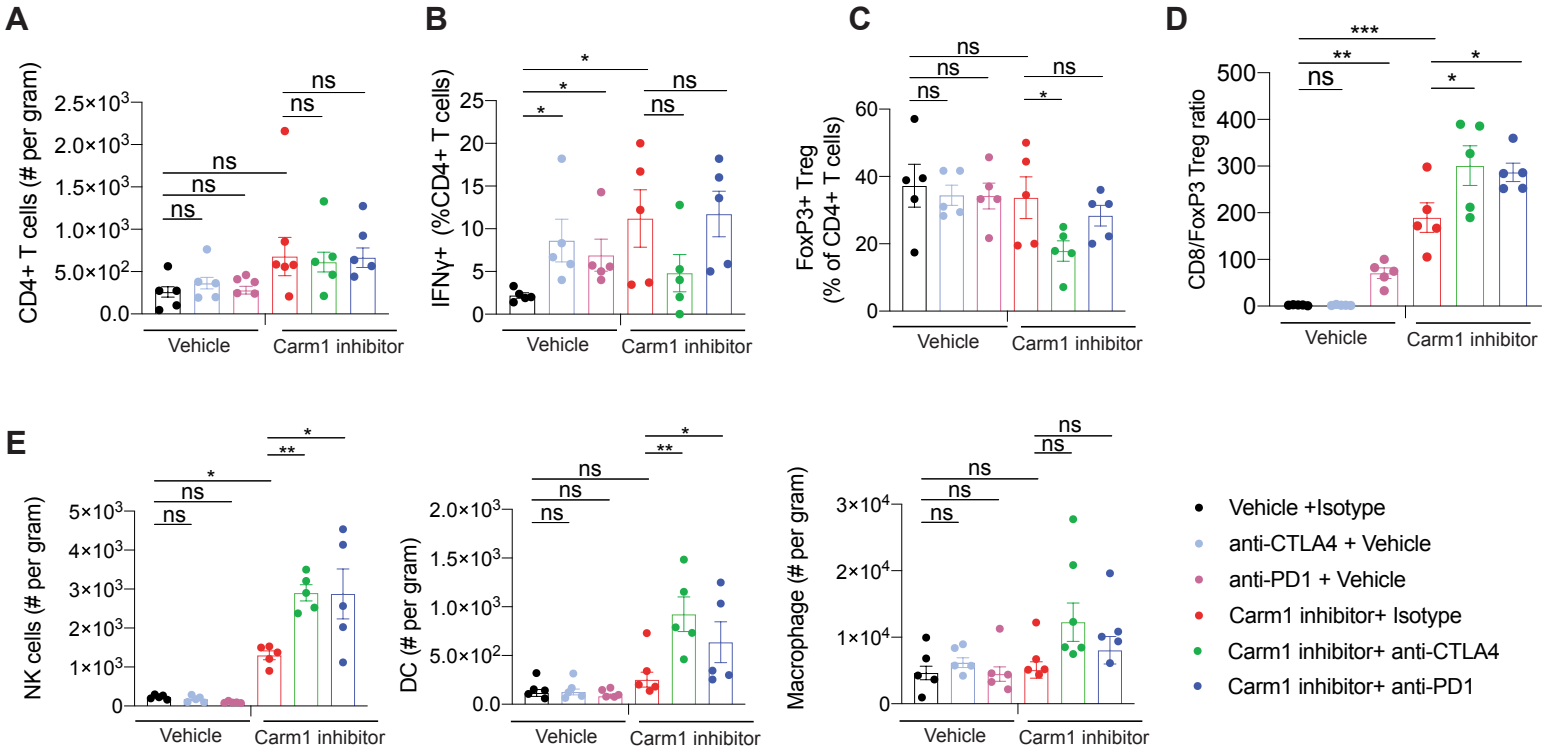
A
CD4+ T cells (# per gram)
2.5×10^3
2.0×10^3
1.5×10^3
1.0×10^3
5.0×10^2
0.0
ns
ns
ns
ns
Vehicle
Carm1 inhibitor
B
IFNγ+ (%CD4+ T cells)
25
20
15
10
5
0
*
*
*
ns
ns
Vehicle
Carm1 inhibitor
C
FoxP3+ Treg
(% of CD4+ T cells)
60
40
20
0
ns
ns
ns
ns
*
Vehicle
Carm1 inhibitor
D
CD8/FoxP3 Treg ratio
500
400
300
200
100
0
***
**
*
ns
*
Vehicle
Carm1 inhibitor
E
NK cells (# per gram)
5×10^3
4×10^3
3×10^3
2×10^3
1×10^3
0
*
**
*
ns
ns
Vehicle
Carm1 inhibitor
DC (# per gram)
2.0×10^3
1.5×10^3
1.0×10^3
5.0×10^2
0.0
*
**
ns
ns
ns
Vehicle
Carm1 inhibitor
Macrophage (# per gram)
3×10^4
2×10^4
1×10^4
0
ns
ns
ns
ns
ns
Vehicle
Carm1 inhibitor
Vehicle +Isotype
anti-CTLA4 + Vehicle
anti-PD1 + Vehicle
Carm1 inhibitor+ Isotype
Carm1 inhibitor+ anti-CTLA4
Carm1 inhibitor+ anti-PD1

**Figure S9. Changes in tumor microenvironment induced by monotherapy or combination therapy with CARM1 inhibitor. Related to Figure 5.**

Treatment of mice with B16F10 melanomas with CARM1 inhibitor or vehicle control. Mice also received isotype control, CTLA-4 or PD-1 mAbs, as indicated (n=5 mice/group).

**A.** Quantification of CD4+ T cells (number per gram of tumor) for the indicated treatment groups.

**B.** Quantification of IFNγ+ cells (as percentage of CD4+ T cells) for the indicated treatment groups.

**C.** Quantification of FoxP3+ Treg cells (as percentage of CD4+ T cells) for the indicated treatment groups.

**D.** Quantification of the CD8/FoxP3 Treg ratio for the indicated treatment groups.

**E.** Number of intra-tumoral NK cells (left), dendritic cells (live, singlet, CD45+ CD3- F4/80- CD11c+ $MHCII^{hi}$) (middle) and macrophages (live, singlet, CD45+ CD3- F4/80+) (right) calculated per gram of tumor.

Figure S10

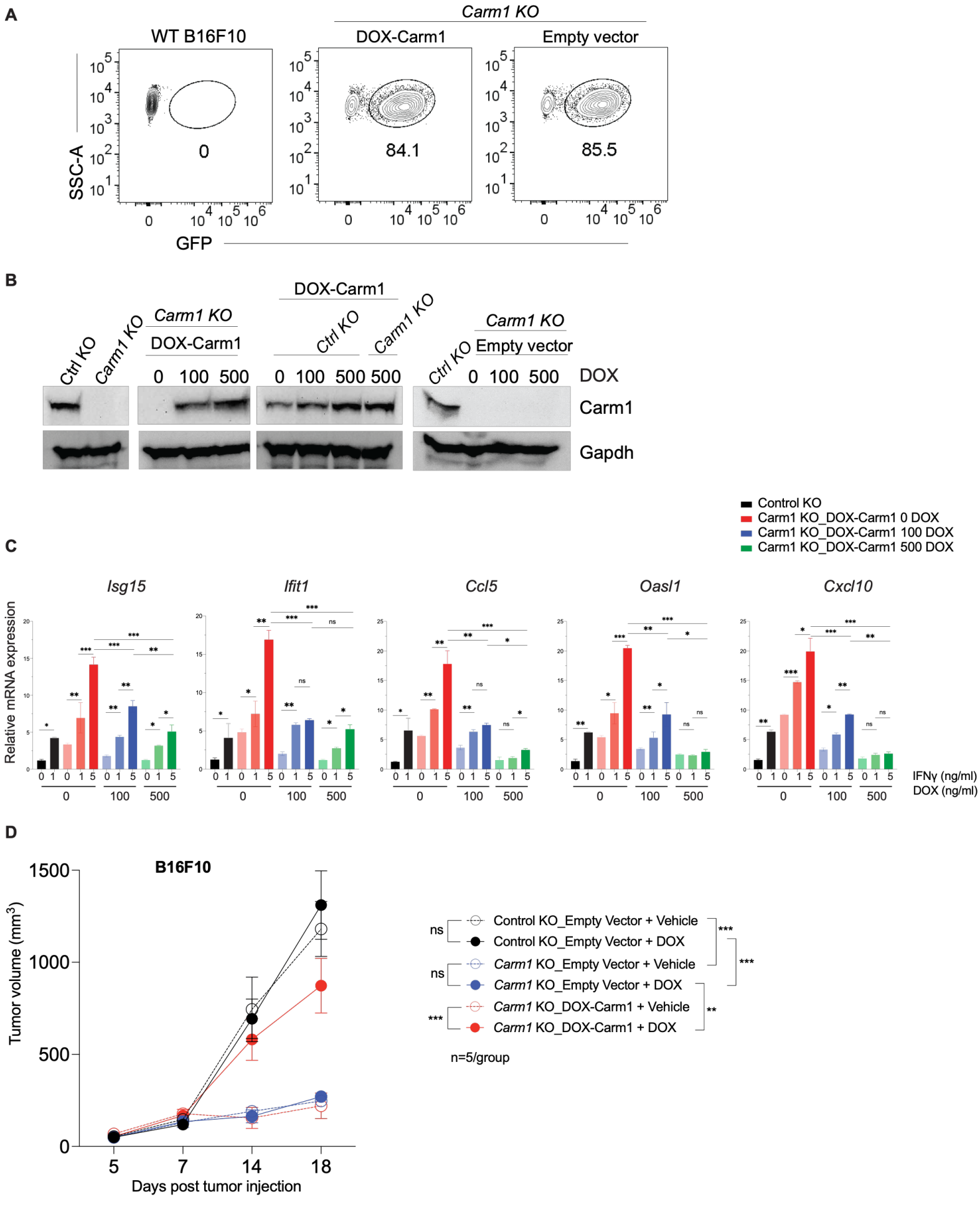
A
Carm1 KO
WT B16F10
DOX-Carm1
Empty vector
SSC-A
GFP
0
84.1
85.5
B
DOX-Carm1
Carm1 KO
Ctrl KO
Carm1 KO
DOX-Carm1
Ctrl KO
Carm1 KO
Carm1 KO
Empty vector
Ctrl KO
0 100 500
0 100 500 500
0 100 500
DOX
Carm1
Gapdh
Control KO
Carm1 KO_DOX-Carm1 0 DOX
Carm1 KO_DOX-Carm1 100 DOX
Carm1 KO_DOX-Carm1 500 DOX
C
Isg15
Ifit1
Ccl5
Oasl1
Cxcl10
Relative mRNA expression
IFNγ (ng/ml)
DOX (ng/ml)
D
B16F10
Tumor volume (mm3)
Days post tumor injection
Control KO_Empty Vector + Vehicle
Control KO_Empty Vector + DOX
Carm1 KO_Empty Vector + Vehicle
Carm1 KO_Empty Vector + DOX
Carm1 KO_DOX-Carm1 + Vehicle
Carm1 KO_DOX-Carm1 + DOX
n=5/group

**Figure S10. Reconstitution of *Carm1* gene expression using a doxycycline-inducible promoter reverses the *Carm1* knockout phenotype. Related to Figure 5.**

**A.** Transduction of *Carm1*-KO B16F10 cells with a lentiviral vector (DOX-Carm1) driving expression of a *Carm1* cDNA under the control of a doxycycline (DOX) inducible promoter. Representative flow plots are shown following sorting of GFP+ cells for tumor cells transduced with DOX-Carm1 or empty vectors.

**B.** Western blot validation of Carm1 protein expression following DOX induction for 7 days in the indicated cell populations. Gapdh is shown as loading control.

**C.** RT-qPCR analysis of selected ISGs. *Carm1*-KO cells expressing the DOX-inducible Carm1 cDNA were treated with doxycycline (0, 100 or 500 ng/ml) for 7 days and then treated overnight with IFNγ (0, 1 or 5 ng/ml) (n=3/group). Control-KO cells not treated with IFNγ were included for comparison.

**D.** Growth of B16F10 melanomas was compared for the following conditions: control-KO tumor cells transduced with the empty vector, *Carm1*-KO tumor cells transduced with the empty vector and *Carm1* KO tumor cells transduced with DOX-Carm1 vector. For each of these groups, mice were fed a regular diet or a doxycycline-containing diet (625ppm, Envigo Teclad) post tumor cell injection until the experimental endpoint (18 days).

Figure S11

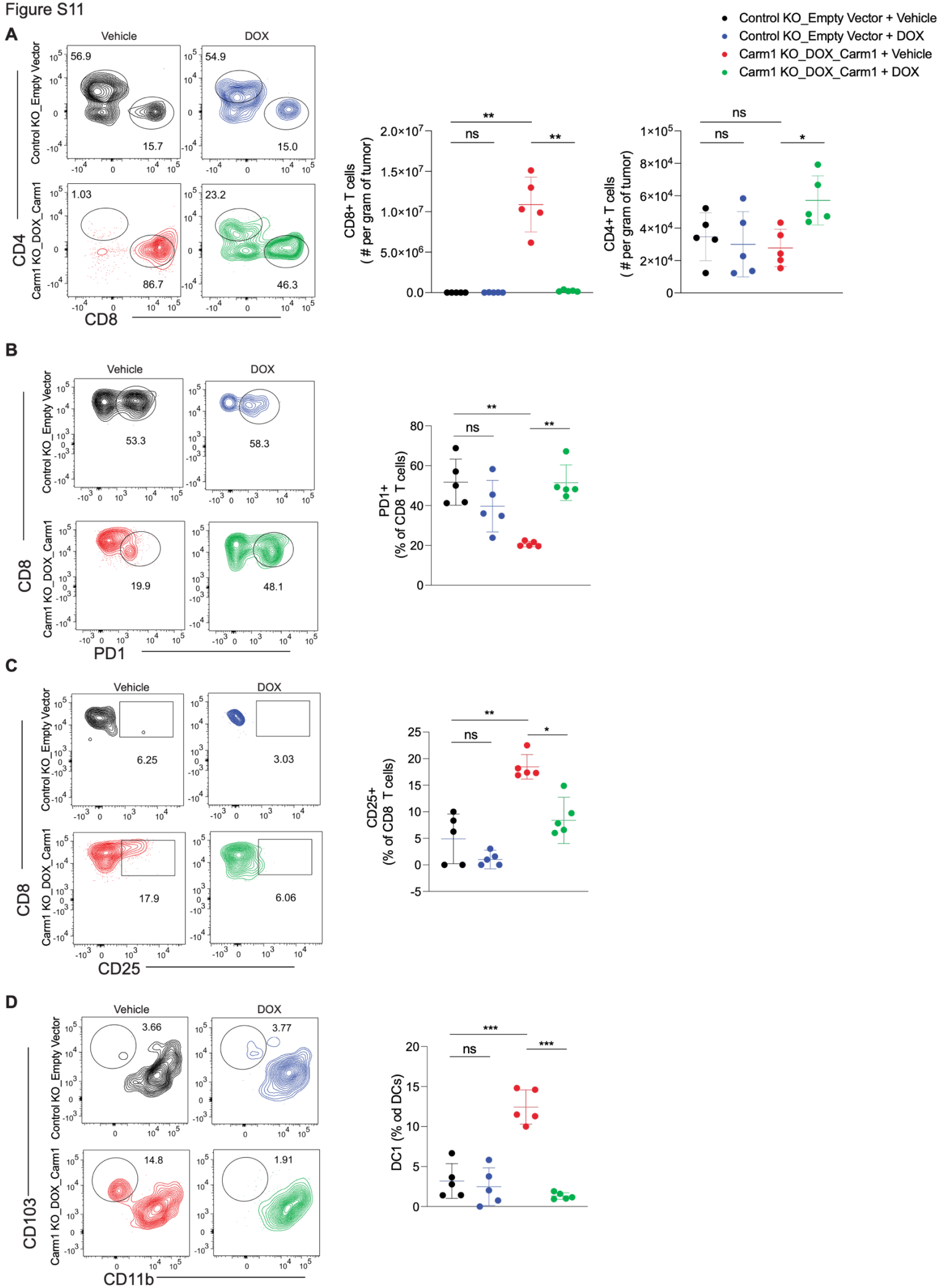
A
Vehicle
DOX
Control KO_Empty Vector
Carm1 KO_DOX_Carm1
CD4
CD8
56.9
15.7
54.9
15.0
1.03
86.7
23.2
46.3
Control KO_Empty Vector + Vehicle
Control KO_Empty Vector + DOX
Carm1 KO_DOX_Carm1 + Vehicle
Carm1 KO_DOX_Carm1 + DOX
CD8+ T cells
( # per gram of tumor)
CD4+ T cells
( # per gram of tumor)
ns
**
*
B
53.3
58.3
19.9
48.1
PD1
PD1+
(% of CD8 T cells)
C
6.25
3.03
17.9
6.06
CD25
CD25+
(% of CD8 T cells)
D
3.66
3.77
14.8
1.91
CD103
CD11b
DC1 (% od DCs)
***

**Figure S11. Reconstitution of *Carm1* gene expression using a doxycycline-inducible promoter reverses the favorable changes in the tumor microenvironment. Related to Figure 5.**

Control-KO B16F10 tumor cells transduced with the empty lentiviral vector or *Carm1*-KO tumor cells expressing the DOX-Carm1 cDNA were implanted into C57Bl/6 mice. Mice with either type of tumor cells were fed a regular diet or a doxycycline-containing diet (625ppm, Envigo Teclad) post tumor cell injection until the experimental endpoint (18 days).

**A.** CD8 and CD4 T cell infiltration was analyzed for the indicated treatment groups (n=5 mice/group). Contour plots show percentage of CD4+ and CD8+ intra-tumoral T cells (left). Summary graphs show quantification of CD8 and CD4 T cells as number per gram of tumor (right).

**B.** Quantification of PD-1+ intra-tumoral CD8+ T cells for the indicated treatment groups (right). Contour plots (left) show percentage of CD8+ PD-1+ positive intra-tumoral T cells, n=5/group.

**C.** Quantification of CD25+ intra-tumoral CD8+ T cells for the indicated treatment groups (right). Contour plots (left) show percentage of CD8+ T cells that are CD25 positive, n=5/group.

**D.** Characterization of intra-tumoral cDC1 cells. Contour plot show percentage of CD103+CD11b- cDC1s (gated on live, singlet, CD45+ CD3- F4/80- CD11c+ MHCIIhi) (left). Summary plot shows percentage of cDC1 (CD103+CD11b-) cells as percentage of total DCs (right), n=5/group.

Figure S12

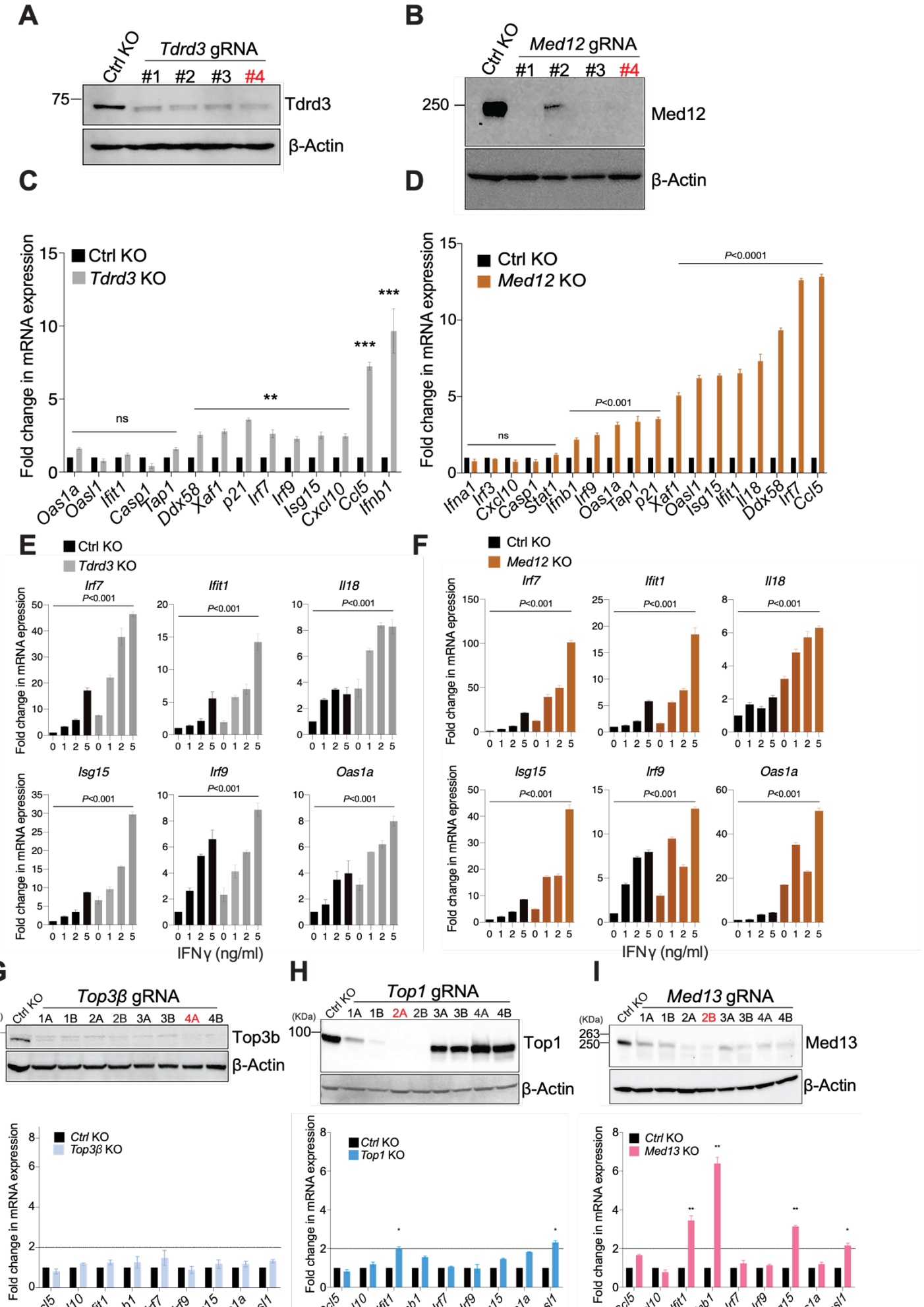
A
Ctrl KO
Tdrd3 gRNA
#1 #2 #3 #4
75
Tdrd3
β-Actin
B
Ctrl KO
Med12 gRNA
#1 #2 #3 #4
250
Med12
β-Actin
C
Ctrl KO
Tdrd3 KO
Fold change in mRNA expression
ns
**
***
***
Oas1a Oasl1 Ifit1 Casp1 Tap1 Ddx58 Xaf1 p21 Irf7 Irf9 Isg15 Cxcl10 Ccl5 Ifnb1
D
Ctrl KO
Med12 KO
P<0.0001
P<0.001
ns
Ifna1 Irf3 Cxcl10 Casp1 Stat1 Ifnb1 Irf9 Oas1a Tap1 p21 Xaf1 Oasl1 Isg15 Ifit1 Il18 Ddx58 Irf7 Ccl5
E
Ctrl KO
Tdrd3 KO
Irf7
Ifit1
Il18
Isg15
Irf9
Oas1a
P<0.001
Fold change in mRNA epression
IFNγ (ng/ml)
F
Ctrl KO
Med12 KO
Irf7
Ifit1
Il18
Isg15
Irf9
Oas1a
P<0.001
Fold change in mRNA epression
IFNγ (ng/ml)
G
Top3β gRNA
Ctrl KO
1A 1B 2A 2B 3A 3B 4A 4B
(KDa)
100
Top3b
β-Actin
Ctrl KO
Top3β KO
Fold change in mRNA expression
Ccl5 Cxcl10 Ifit1 Ifnb1 Irf7 Irf9 Isg15 Oas1a Oasl1
H
Top1 gRNA
Ctrl KO
1A 1B 2A 2B 3A 3B 4A 4B
(KDa)
100
Top1
β-Actin
Ctrl KO
Top1 KO
Fold change in mRNA expression
Ccl5 Cxcl10 Ifit1 Ifnb1 Irf7 Irf9 Isg15 Oas1a Oasl1
I
Med13 gRNA
Ctrl KO
1A 1B 2A 2B 3A 3B 4A 4B
(KDa)
263
250
Med13
β-Actin
Ctrl KO
Med13 KO
Fold change in mRNA expression
Ccl5 Cxcl10 Ifit1 Ifnb1 Irf7 Irf9 Isg15 Oas1a Oasl1

**Figure S12. Inactivation of *Tdrd3* and *Med12* genes results in a similar phenotype as inactivation of *Carm1* gene. Related to Figure 6.**

**A.** Tdrd3 protein levels in B16F10 cells edited with *Tdrd3* or control (Ctrl) gRNAs. Replicates of different lines edited with same gRNA are shown. Cell line highlighted in red was used for experiments.

**B.** Med12 protein levels in B16F10 cells edited with *Med12* or control gRNAs. Replicates of different lines edited with the same gRNA are shown.

**C.** RT-qPCR analysis of selected ISGs and IFNs in *Tdrd3*-KO and control-KO B16F10 cells (n=4/group).

**D.** RT-qPCR analysis of transcripts of selected ISGs and IFNs in *Med12*-KO and control-KO B16F10 cells (n=4/group).

**E.** Response of *Tdrd3*-KO and control-KO B16F10 cells to IFNγ stimulation. RT-qPCR analysis of transcripts of selected ISGs and IFNs following overnight stimulation with the indicated concentrations of IFNγ (n=4/group).

**F.** Response of *Med12-KO* and control-KO B16F10 cells to IFNγ stimulation. RT-qPCR analysis of transcripts of selected ISGs and IFNs following overnight stimulation with the indicated concentrations of IFNγ (n=4/group).

**G-I.** Western blot validation of *Top3b* **(G)**, *Top1* **(H)** and *Med13* **(I)** editing in B16F10 cells. RT-qPCR analysis was performed for selected ISGs and IFNs in indicated cell lines (bottom) (n=4/group).

Data shown are representative of two independent experiments with 4 replicates/group. Mann-Whitney test was used to determine significance, ***P < 0.001; **P < 0.01; *P < 0.05; n.s., not significant.

Figure S13

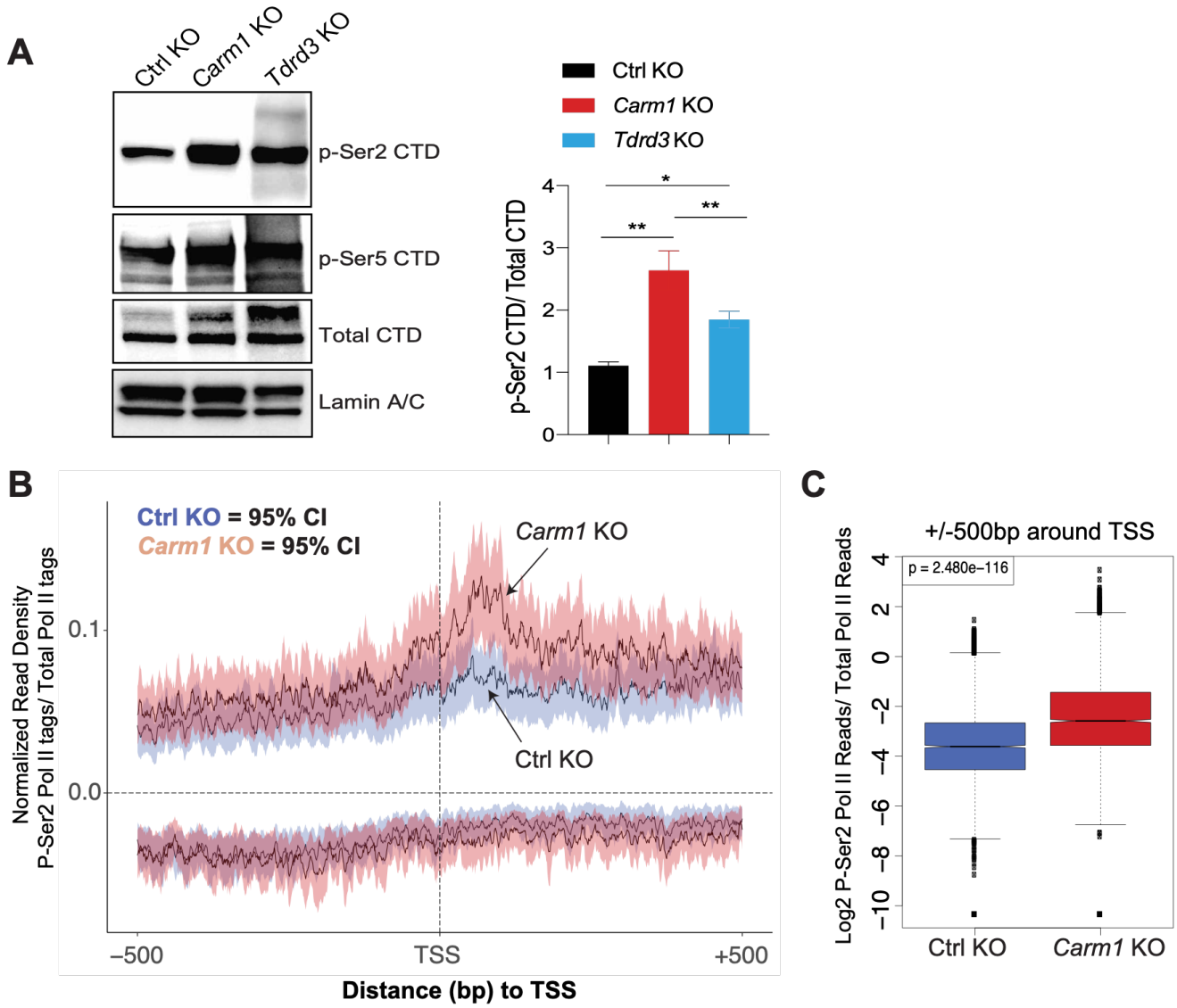
A
Ctrl KO
Carm1 KO
Tdrd3 KO
p-Ser2 CTD
p-Ser5 CTD
Total CTD
Lamin A/C
Ctrl KO
Carm1 KO
Tdrd3 KO
p-Ser2 CTD/ Total CTD
B
Ctrl KO = 95% CI
Carm1 KO = 95% CI
Carm1 KO
Ctrl KO
Normalized Read Density
P-Ser2 Pol II tags/ Total Pol II tags
–500
TSS
+500
Distance (bp) to TSS
C
+/-500bp around TSS
p = 2.480e–116
Log2 P-Ser2 Pol II Reads/ Total Pol II Reads
Ctrl KO
Carm1 KO
D
Genes enriched in Carm1 KO cells
2276
223
919
mNETSeq
RNASeq
E
Pathways enriched in Carm1 KO cells
mNETSeq
E2F targets
G2M checkoints
Mitotic spindle
DNA repair
p53 pathway
p<0.00001
-Log10 (FDR)
Overlapping (mNETSeq-RNASeq)
Oxidative phosphorylation
p53 pathway
TNFA signaling via NFkB
UV response UP
IL2 STAT5 signaling
p<0.00001
-Log10 (FDR)
F
Pathways of differentially spliced genes in Carm1 KO tumor cells
DNA repair
Protein phosphorylation
cytoskeleton organization
cytoskeleton organization
DNA repair
Cell cycle
Regulation of GTPase activity
Regulation of transcription
Chromatin organization
exon gains
(n=638 genes)
exon losses
(n=708 genes)
-Log2 (p-value)
G
Metaplot for DRIP-seq
Log2 FC Carm1 KO vs WT
Mean of normalized count

**Figure S13. Alterations in transcription in *Carm1*-KO tumor cells. Related to Figure 6.**

**A.** Western blot analysis of nuclear lysates from control-KO, *Carm1*-KO or *Tdrd3*-KO B16F10 cells. Equal quantities of nuclear protein extracts from indicated cell lines were probed using antibodies specific for phosphorylated (p-Ser2 CTD and p-Ser5) or non-phosphorylated (total) C-terminal domain of RNA Pol II (CTD). Lamin A/C was used as loading control (left). Fraction of phosphorylated RNA Pol II was estimated by normalizing p-Ser2 CTD to total CTD levels (right). Data shown are representative of three experiments.

**B.** Ratio of normalized P-Ser2 Pol II and total Pol II mNET-Seq signals within 500 bp of transcription start sites (TSS) of expressed protein-encoding genes in *Carm1*-KO (red) and control-KO (blue) cells. Shaded region indicates a 95% confidence interval.

**C.** Boxplots representing the ratio of P-Ser2 Pol II to total Pol II mNET-Seq reads within 500 bp of TSS in *Carm1*-KO (red) and in control-KO (blue) cells.

**D.** Venn diagram showing overlap between genes with increased normalized P-Ser2 RNA Pol II reads (shown as mNETSeq, blue) and genes with higher expression (shown as RNASeq, red) in *Carm1*-KO relative to control-KO B16F10 cells.

**E.** Top enriched pathways from GSEA analysis of genes with increased normalized P-Ser2 RNA Pol II reads (all 2,837 mNETSeq genes, blue) (left) in *Carm1*-KO compared to control-KO B16F10 cells. GSEA analysis for 275 overlapping genes between mNETSeq and RNASeq (right).

**F.** Pathway analysis of differentially spliced genes in *Carm1-KO* tumor cells. Differential splicing analysis was conducted using DESeq2 using log2(FC) greater than 2-fold and adjusted p-value < 0.05) as statistical thresholds. Enriched gene ontologies were identified using the String Database. Number of exon gains and losses are shown in inset.

**G.** Metaplot for DRIPseq (DNA-RNA immunoprecipitation analysis) representing the log2 fold change in mean normalized count of peaks in *Carm1*-KO and control-KO cells.

Figure S14

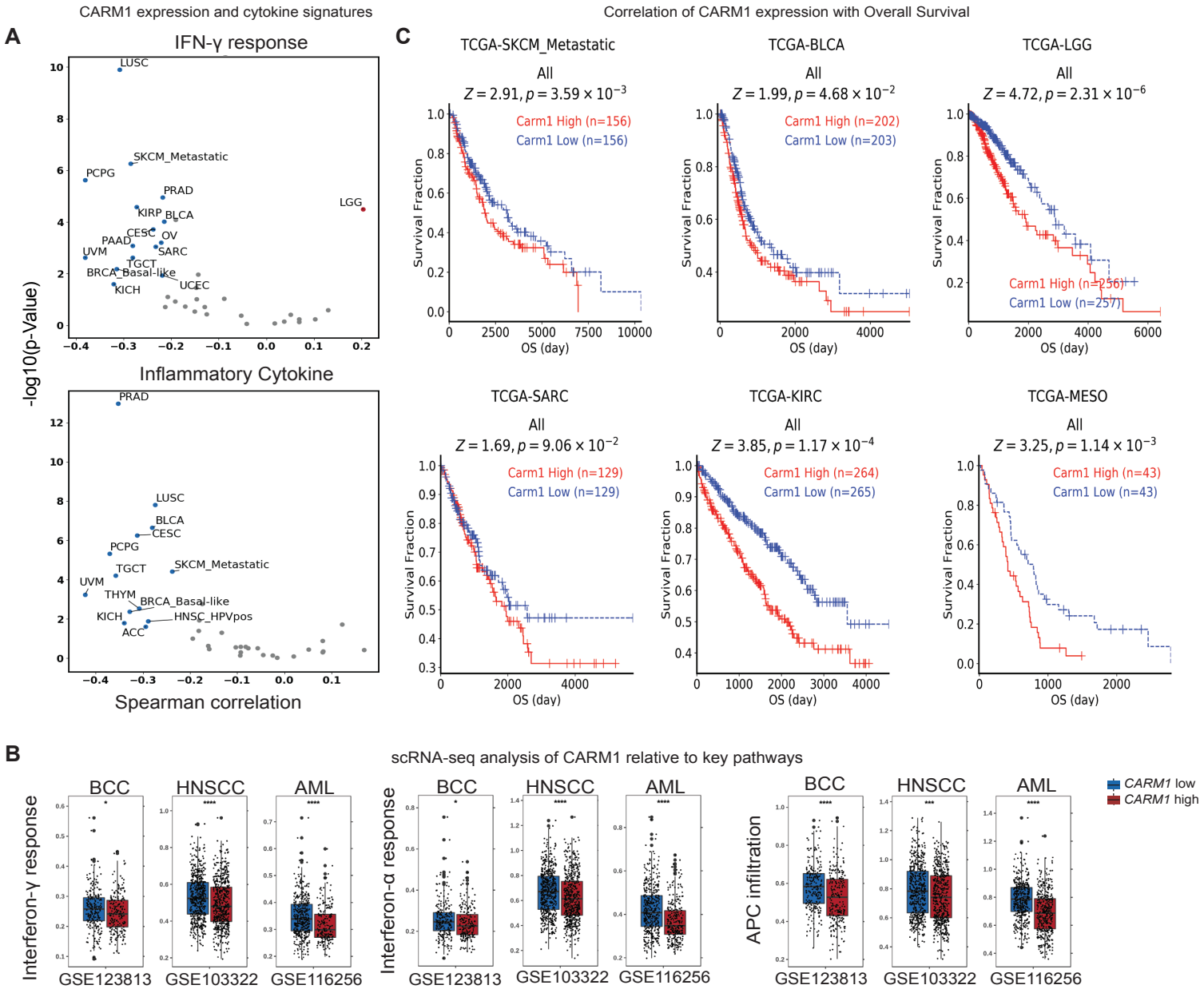
CARM1 expression and cytokine signatures
A
IFN-γ response
-log10(p-Value)
LUSC
SKCM_Metastatic
PCPG
PRAD
LGG
KIRP
BLCA
CESC
OV
PAAD
SARC
UVM
TGCT
BRCA_Basal-like
UCEC
KICH
Inflammatory Cytokine
PRAD
LUSC
BLCA
CESC
PCPG
TGCT
SKCM_Metastatic
UVM
THYM
BRCA_Basal-like
KICH
HNSC_HPVpos
ACC
Spearman correlation
Correlation of CARM1 expression with Overall Survival
C
TCGA-SKCM_Metastatic
All
Z = 2.91, p = 3.59 × 10−3
Carm1 High (n=156)
Carm1 Low (n=156)
TCGA-BLCA
All
Z = 1.99, p = 4.68 × 10−2
Carm1 High (n=202)
Carm1 Low (n=203)
TCGA-LGG
All
Z = 4.72, p = 2.31 × 10−6
Carm1 High (n=256)
Carm1 Low (n=257)
TCGA-SARC
All
Z = 1.69, p = 9.06 × 10−2
Carm1 High (n=129)
Carm1 Low (n=129)
TCGA-KIRC
All
Z = 3.85, p = 1.17 × 10−4
Carm1 High (n=264)
Carm1 Low (n=265)
TCGA-MESO
All
Z = 3.25, p = 1.14 × 10−3
Carm1 High (n=43)
Carm1 Low (n=43)
Survival Fraction
OS (day)
B
scRNA-seq analysis of CARM1 relative to key pathways
Interferon-γ response
Interferon-α response
APC infiltration
BCC
HNSCC
AML
GSE123813
GSE103322
GSE116256
CARM1 low
CARM1 high

**Figure S14. Expression of *CARM1* in human cancers. Related to Figure 7.**

**A.** Analysis of TCGA RNA-seq data across human cancer types. Correlation of *CARM1* mRNA levels with indicated pathways. Plots show Spearman's correlation and estimated statistical significance for indicated pathways in different cancer types adjusted for tumor purity. Each dot represents a cancer type in TCGA.

**B.** Analysis of scRNA-seq data of malignant cells from three human cancer cohorts (GSE123813: basal cell carcinoma; GSE103322: head and neck cancer; GSE116256: AML). Scores for IFN-γ response, IFN-α response and APC (antigen presentation cell infiltration) pathways are shown. Data were stratified by *CARM1* high and low groups using median expression levels. Statistical comparisons were made using two-sided unpaired Mann-Whitney tests.

**C.** Association of *CARM1* mRNA levels with survival in metastatic melanoma (SKCM), bladder urothelial carcinoma (BLCA), Low Grade Glioma (LGG), sarcoma (SARC), Kidney Renal Clear Cell Carcinoma (KIRC), Mesothelioma (MESO). A total of 12 TCGA datasets were analyzed. Statistical analysis was performed using TIMER2.0; shown are all cancer types in which *CARM1* mRNA levels correlated with survival.

Figure S15

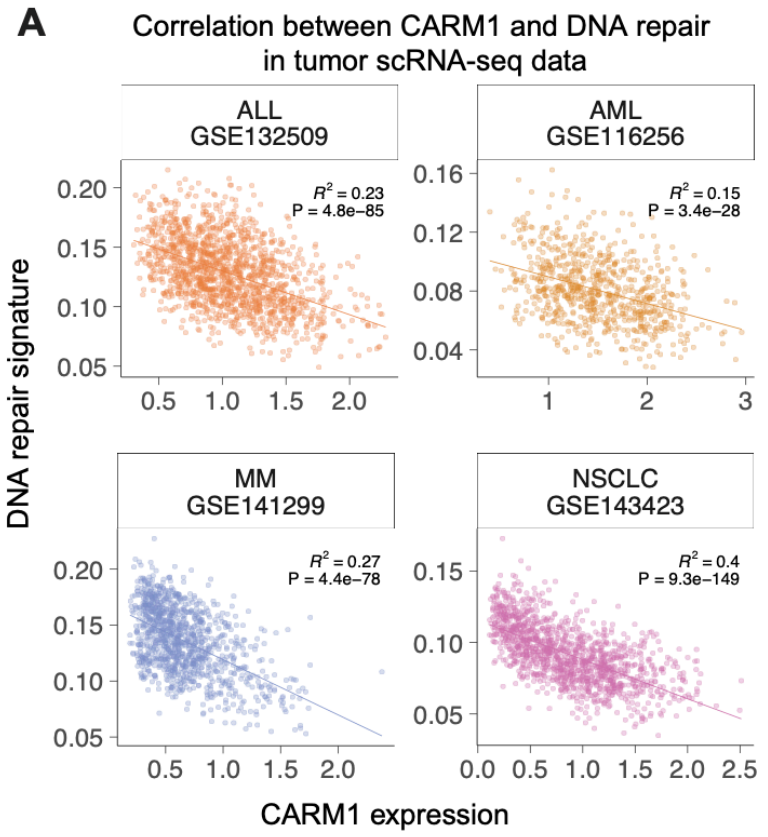
A
Correlation between CARM1 and DNA repair
in tumor scRNA-seq data
ALL
GSE132509
$R^2$ = 0.23
P = 4.8e−85
AML
GSE116256
$R^2$ = 0.15
P = 3.4e−28
MM
GSE141299
$R^2$ = 0.27
P = 4.4e−78
NSCLC
GSE143423
$R^2$ = 0.4
P = 9.3e−149
DNA repair signature
CARM1 expression

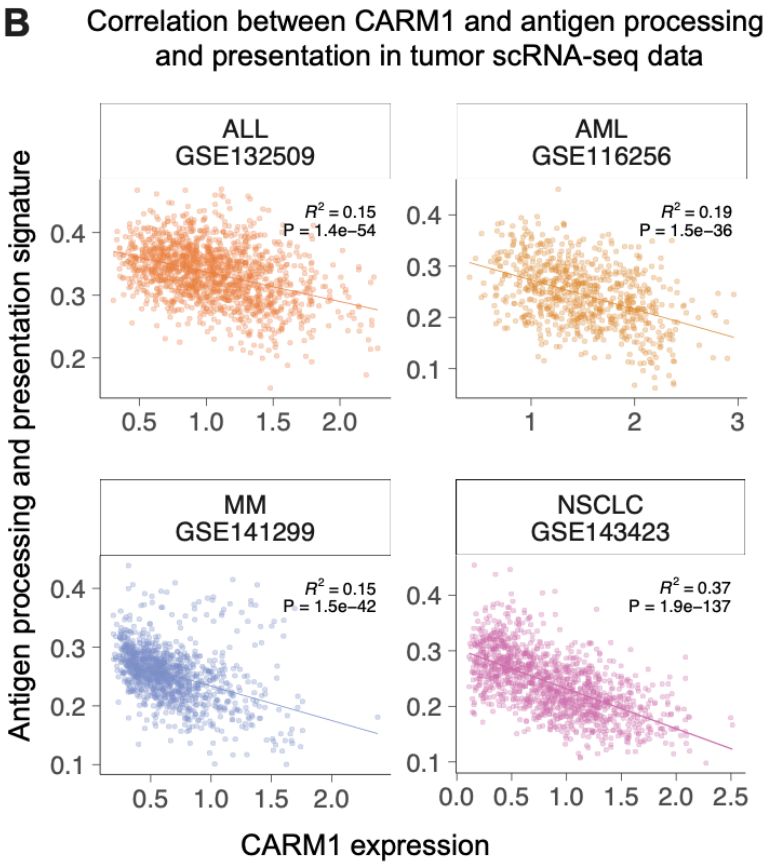
B
Correlation between CARM1 and antigen processing
and presentation in tumor scRNA-seq data
ALL
GSE132509
$R^2$ = 0.15
P = 1.4e−54
AML
GSE116256
$R^2$ = 0.19
P = 1.5e−36
MM
GSE141299
$R^2$ = 0.15
P = 1.5e−42
NSCLC
GSE143423
$R^2$ = 0.37
P = 1.9e−137
Antigen processing and presentation signature
CARM1 expression

**Figure S15. Single cell analysis of human tumor cells for correlation between *CARM1* mRNA expression and DNA repair as well as antigen presentation pathways. Related to Figure 7.**

**A-B.** Single-cell RNA-seq data of malignant cells were investigated for correlation between *CARM1* mRNA expression and DNA repair pathway hallmark genes (msigdb/hallmark: DNA Repair) **(A)** as well as antigen processing and presentation pathway (KEGG: https://www.genome.jp/kegg-bin/show_pathway?hsa04612) **(B)**. Data are shown for the following human scRNA-seq datasets: ALL (Acute Lymphoblastic Leukemia), AML (Acute Myeloid Leukemia), MM (Multiple Myeloma) and NSCLC (Non-Small Cell Lung Cancer).

Figure S16

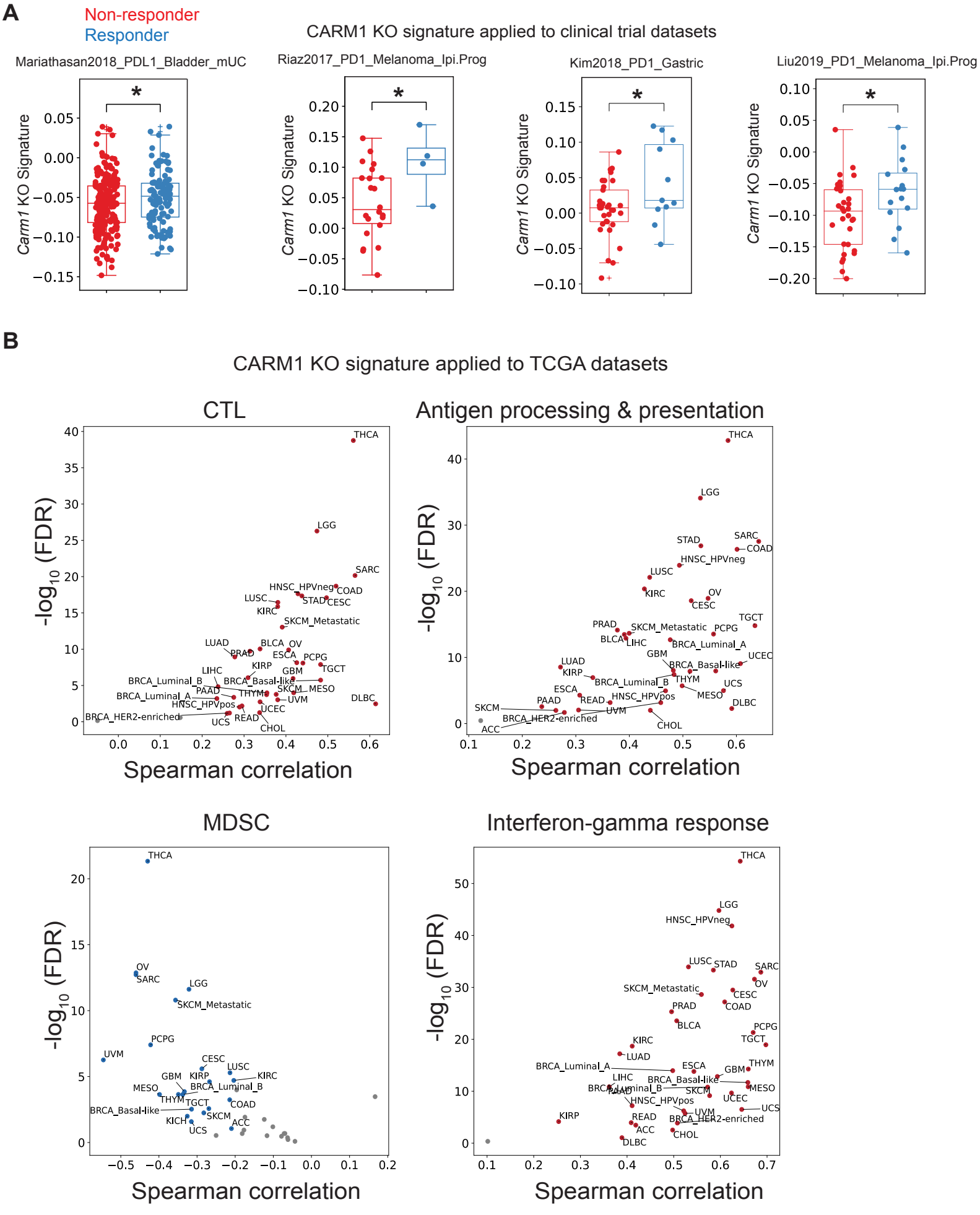
A
Non-responder
Responder
CARM1 KO signature applied to clinical trial datasets
Mariathasan2018_PDL1_Bladder_mUC
Riaz2017_PD1_Melanoma_Ipi.Prog
Kim2018_PD1_Gastric
Liu2019_PD1_Melanoma_Ipi.Prog
Carm1 KO Signature
*
B
CARM1 KO signature applied to TCGA datasets
CTL
Antigen processing & presentation
MDSC
Interferon-gamma response
-log10 (FDR)
Spearman correlation
THCA
LGG
SARC
HNSC_HPVneg
COAD
LUSC
STAD
CESC
KIRC
SKCM_Metastatic
LUAD
BLCA
OV
PRAD
ESCA
PCPG
LIHC
KIRP
GBM
TGCT
BRCA_Luminal_B
BRCA_Basal-like
SKCM
MESO
PAAD
THYM
BRCA_Luminal_A
UVM
HNSC_HPVpos
DLBC
UCEC
BRCA_HER2-enriched
UCS
READ
CHOL
ACC
SKCM
KICH

**Figure S16. Analysis of *CARM1* KO gene expression signature for ICB response in clinical trials and immune-related pathways. Related to Figure 7.**

**A.** *CARM1* KO gene signature levels in indicated ICB (immune checkpoint blockade) cohorts of responder and non-responder patients enrolled in clinical trials evaluating PD-1 or PD-L1 blocking mAbs. In each subgroup, predictive power of ICB response was evaluated by comparing *CARM1* KO gene signature high and low groups. The p-values were inferred by Mann-Whitney U test. *p-value<0.1; NS (non-significant). Ipi (Ipilimumab).

**B.** Analysis of *CARM1* KO signature in TCGA RNA-seq datasets across human cancer types. Correlation of *CARM1* KO signature with indicated immune-related pathways. Plots show Spearman's correlation and estimated statistical significance for indicated pathways in different cancer types adjusted for tumor purity. Each dot represents a cancer type in TCGA.

**Supplemental references of ICB clinical data:**


1. Gide TN, Quek C, Menzies AM, Tasker AT, Shang P, Holst J*, et al.* Distinct immune cell populations define response to anti-PD-1 monotherapy and anti-PD-1/anti-CTLA-4 combined therapy. Cancer cell **2019**;35(2):238-55. e6.

2. Kim ST, Cristescu R, Bass AJ, Kim K-M, Odegaard JI, Kim K*, et al.* Comprehensive molecular characterization of clinical responses to PD-1 inhibition in metastatic gastric cancer. Nature medicine **2018**;24(9):1449-58.

3. Liu D, Schilling B, Liu D, Sucker A, Livingstone E, Jerby-Amon L*, et al.* Integrative molecular and clinical modeling of clinical outcomes to PD1 blockade in patients with metastatic melanoma. Nature medicine **2019**;25(12):1916-27.

4. Mariathasan S, Turley SJ, Nickles D, Castiglioni A, Yuen K, Wang Y*, et al.* TGFβ attenuates tumour response to PD-L1 blockade by contributing to exclusion of T cells. Nature **2018**;554(7693):544-8.

5. McDermott DF, Huseni MA, Atkins MB, Motzer RJ, Rini BI, Escudier B*, et al.* Clinical activity and molecular correlates of response to atezolizumab alone or in combination with bevacizumab versus sunitinib in renal cell carcinoma. Nature medicine **2018**;24(6):749-57.

6. Riaz N, Havel JJ, Makarov V, Desrichard A, Urba WJ, Sims JS*, et al.* Tumor and microenvironment evolution during immunotherapy with nivolumab. Cell **2017**;171(4):934-49. e16.

7. Zhao J, Chen AX, Gartrell RD, Silverman AM, Aparicio L, Chu T*, et al.* Immune and genomic correlates of response to anti-PD-1 immunotherapy in glioblastoma. Nature medicine **2019**;25(3):462-9.